



# Extreme storms cause rapid but short lived shifts in nearshore subtropical bacterial communities

Author	Angela Ares, Margaret Mars Brisbin, Kirk N. Sato, Juan P. Martin, Yoshiteru Iinuma, Satoshi Mitarai
journal or publication title	Environmental Microbiology
volume	22
number	11
page range	4571-4588
year	2020-08-23
Publisher	Society for Applied Microbiology and John Wiley & Sons
Rights	This is the peer reviewed version of the following article: Ares, A., Brisbin, M.M., Sato, K.N., Martin, J.P., Iinuma, Y. and Mitarai, S. (2020), Extreme storms cause rapid but short lived shifts in nearshore subtropical bacterial communities. Environ Microbiol, 22: 4571-4588., which has been published in final form at <a href="https://doi.org/10.1111/1462-2920.15178">https://doi.org/10.1111/1462-2920.15178</a> . This article may be used for non-commercial purposes in accordance with Wiley Terms and Conditions for Use of Self-Archived Versions.
Author's flag	author
URL	<a href="http://id.nii.ac.jp/1394/00001640/">http://id.nii.ac.jp/1394/00001640/</a>

doi: info:doi/10.1111/1462-2920.15178

1 **Extreme storms cause rapid but short-lived shifts in nearshore subtropical bacterial**  
2 **communities**

3  
4

5 Ángela Ares<sup>1\*</sup>, Margaret Mars Brisbin<sup>1\*</sup>, Kirk N. Sato<sup>1,2</sup>, Juan P. Martín<sup>1</sup>, Yoshiteru Inuma<sup>3</sup>,  
6 Satoshi Mitarai<sup>1</sup>

7  
8 \* contributed equally  
9

10 <sup>1</sup> Marine Biophysics Unit, Okinawa Institute of Science and Technology (OIST, Okinawa, Japan)

11 <sup>2</sup> Friday Harbor Laboratories, University of Washington (U.S.A.)

12 <sup>3</sup> Instrumental Analysis Section, Okinawa Institute of Science and Technology (OIST, Okinawa, Japan)

13  
14

15 **Originality-Significance Statement**

16

17 Extreme storm events, such as tropical cyclones, can negatively affect coastal ecosystems  
18 through increased terrestrial run-off, pollution, and physical destruction. Future climate  
19 scenarios predict increased frequency and intensity of tropical cyclones, necessitating a better  
20 understanding of how ecosystems respond to such events. In this study, we show the short-  
21 term dynamics of nearshore bacterial communities during two major tropical cyclones occurring  
22 at the beginning and end of the typhoon season in the subtropical western Pacific. Importantly,  
23 field observations were coupled with concurrent mesocosm experiments to isolate the effects of  
24 terrestrial sediment input from other storm effects, such as wind, waves, and fresh-water influx.  
25 Our study reveals that shifts in bacterial communities in both instances were extremely rapid but  
26 highly context dependent.

27  
28

29 **Abstract**

30

31 Climate change scenarios predict tropical cyclones will increase in both frequency and intensity,  
32 which will escalate the amount of terrestrial run-off and mechanical disruption affecting coastal  
33 ecosystems. Bacteria are key contributors to ecosystem functioning, but relatively little is known

34 about how they respond to extreme storm events, particularly in nearshore subtropical regions.  
35 In this study, we combine field observations and mesocosm experiments to assess bacterial  
36 community dynamics and changes in physicochemical properties during early- and late-season  
37 tropical cyclones affecting Okinawa, Japan. Storms caused large and fast influxes of freshwater  
38 and terrestrial sediment—locally known as red soil pollution—and caused moderate increases  
39 of macronutrients, especially  $\text{SiO}_2$  and  $\text{PO}_4^{3-}$ , with up to 25 and 0.5  $\mu\text{M}$ , respectively. We  
40 detected shifts in relative abundances of marine and terrestrially-derived bacteria, including  
41 putative coral and human pathogens, during storm events. Soil input alone did not substantially  
42 affect marine bacterial communities in mesocosms, indicating that other components of run-off  
43 or other storm effects likely exert a larger influence on bacterial communities. The storm effects  
44 were short-lived and bacterial communities quickly recovered following both storm events. The  
45 early- and late-season storms caused different physicochemical and bacterial community  
46 changes, demonstrating the context-dependency of extreme storm responses in a subtropical  
47 coastal ecosystem.

48

#### 49 **Keywords**

50 Tropical cyclones, typhoons, hurricanes, extreme events, bacterioplankton, coastal, nearshore,  
51 community dynamics, soil pollution, run-off

52

#### 53 **Introduction**

54

55 Extreme storm events, such as tropical cyclones (i.e. tropical storms, hurricanes, and typhoons),  
56 can have dramatic consequences on coastal ecosystems, due in part to the effects of  
57 terrestrially-derived pollution (Hennessy *et al.*, 1997; De Jesus Crespo *et al.*, 2019). In addition  
58 to influencing salinity and turbidity, flood plumes often include elevated concentrations of  
59 bacteria (Solo-Gabriele *et al.*, 2000), nutrients (i.e. C, N, P) (Chen *et al.*, 2012, 2018; Gao *et al.*,

60 2014; Paerl *et al.*, 2018) and other chemicals, such as herbicides or heavy metals (Lewis *et al.*,  
61 2012; Mistri *et al.*, 2019), which can act synergistically to negatively affect coastal ecosystems  
62 (Wooldridge, 2009; Brodie *et al.*, 2012; Lewis *et al.*, 2012). Especially in tropical and subtropical  
63 regions experiencing severe seasonal storms, large volumes of terrestrial run-off entering  
64 coastal waters can degrade coastal ecosystems, including coral reefs, through sedimentation or  
65 disease (Riegl and Branch, 1995; Philipp and Fabricius, 2003; Voss and Richardson, 2006;  
66 Haapkylä *et al.*, 2011; Wilson *et al.*, 2012). Such run-off events can also cause harm more  
67 indirectly, through eutrophication, hypoxia (Fabricius, 2005; Altieri *et al.*, 2017) and decreased  
68 water quality. As global climate change is expected to enhance the frequency and intensity of  
69 extreme storm events (Groisman *et al.*, 2005), it is increasingly important to better understand  
70 how such storms impact coastal ecosystem functioning.

71  
72 The western North Pacific, where there is an average of 27 named storms per year (Wang *et al.*  
73 *et al.*, 2010; Herbeck *et al.*, 2011), is the most active region in the world for tropical cyclones.  
74 Landfalling typhoons, which most affect coastal ecosystems, have intensified in the region; the  
75 proportion of category 4 and 5 typhoons striking land more than doubled in the last four  
76 decades. Current climate models predict continued intensification of landfalling typhoons  
77 affecting mainland China, Taiwan, Korea and Japan, indicating these regions will suffer even  
78 more storm-caused losses of life, property, and coastal habitat (Mei and Xie, 2016). Okinawa  
79 Island—the largest island of the Ryukyu archipelago at the edge of the western North Pacific—  
80 is an ideal natural laboratory for studying storm effects on coastal ecosystems (Figure 1).  
81 Okinawa’s coral reefs have experienced significant declines in recent decades, due in part to  
82 increased storm induced run-off and sedimentation (Omori, 2011; Hongo and Yamano, 2013;  
83 Harii *et al.*, 2014), which is exacerbated by agricultural practices and large coastal development  
84 projects (Omija, 2004; Masucci and Reimer, 2019). The fine-particle, laterite soils with high iron  
85 concentrations found in Okinawa and typical to the region are easily suspended and turn coastal

86 waters a deep, cloudy red color during the frequent tropical cyclones (Supplemental Figure 1)  
87 (Omija, 2004). These events are locally referred to as Red Soil Pollution (Omori, 2011).  
88

89 While the biological consequences of storm-induced run-off have been investigated for corals  
90 and fish species in Okinawa (Hongo and Yamano, 2013; Inoue *et al.*, 2014; Yamazaki *et al.*,  
91 2015; O'Connor *et al.*, 2016; Yamano and Watanabe, 2016), less is known about how tropical  
92 cyclones and associated run-off affects coastal microbial communities and especially bacteria  
93 (Blanco *et al.*, 2008). Microbial communities contribute to marine ecosystems through primary  
94 production and by recycling dissolved organic carbon and nutrients through the microbial loop  
95 (Azam *et al.*, 1983), but can also draw down dissolved oxygen (Anderson and Taylor, 2001) or  
96 cause opportunistic infections in marine organisms (Shinn *et al.*, 2000; Sutherland *et al.*, 2011;  
97 Sheridan *et al.*, 2014; Peters, 2015). Therefore, changes in microbial community compositions  
98 in response to storms could precipitate large-scale ecosystem effects. Microbial responses can  
99 occur extremely quickly; Gammaproteobacteria, Flavobacteria and many Alphaproteobacteria  
100 can increase in abundance within hours when exposed to high nutrient concentrations, whereas  
101 the entire microbial community—including archaea, protists, and viruses—can turn over on the  
102 scale of less than one day to about a week (Fuhrman *et al.*, 2015). Rapid microbial response  
103 times to changing environmental conditions make microbes valuable early-warning bioindicators  
104 (Glasl *et al.*, 2017; Pearman *et al.*, 2018), but also hinders their study. Sampling at the scale of  
105 microbial response times during tropical cyclones is often dangerous and is further complicated  
106 by the poor predictability of storm tracks and intensities (Zhou *et al.*, 2012).  
107

108 In this study, we characterize nearshore bacterial community dynamics in response to tropical  
109 cyclones affecting Okinawa Island and isolate the effects of sediment input through controlled  
110 mesocosm experiments. The study included tropical storm Gaemi at the start of the 2018  
111 Okinawa typhoon season (June 16) and successive category 5 super typhoons, Trami and

112 Kong-Rey, on September 30 and October 5, towards the end of the 2018 season. We evaluated  
113 physicochemical properties and bacterial community compositions in seawater samples  
114 collected before, during/between, and after storms in June and October and in samples taken  
115 from mesocosms with and without red soil amendment. The specific aims for this study were to:  
116 i) assess how bacterial community composition and physicochemical parameters respond in  
117 time to tropical cyclones and sediment input, ii) evaluate the speed of the responses and  
118 recovery, and iii) identify potential ecosystem consequences due to extreme storms and  
119 sediment input.

120

## 121 **Results**

122

### 123 **Physicochemical responses to extreme storm events and red soil input**

124

125 Two major storm events affecting Okinawa Island were monitored for this study. The first event  
126 included tropical storm Gaemi, which made landfall on June 16 and was the first tropical cyclone  
127 of the 2018 typhoon season. Gaemi brought 133.72 mm day<sup>-1</sup> of precipitation and maximum  
128 wind speeds of 12.1 m s<sup>-1</sup> to Okinawa (Figure 2). Substantial precipitation and wind were also  
129 recorded during the two days leading up to Gaemi's landfall (69.77 and 83.99 mm day<sup>-1</sup>  
130 precipitation and 10.2 and 12.1 m s<sup>-1</sup> wind intensity on June 14 and 15, respectively), but no  
131 additional rain was recorded until July (Figure 2). The second event included two category 5  
132 super-typhoons, Trami and Kong-Rey, which impacted Okinawa in rapid succession towards the  
133 end of the 2018 season (Sept. 29 and Oct. 5). Trami and Kong-Rey caused accumulated rainfall  
134 of 239.24 and 87.89 mm day<sup>-1</sup> and maximum wind speeds of 26.9 and 12.7 m s<sup>-1</sup>, respectively.  
135 The June and October events represented the two largest rainfalls during the 2018 typhoon  
136 season, and typhoon Trami recorded the most extreme sustained and gusting wind speeds in  
137 2018 (Figure 2). The extreme winds accompanying Trami and Kong-Rey also caused large

138 waves; Trami and Kong-Rey both brought waves with heights greater than nine meters (Japan  
139 Meteorological Agency, [https://www.data.jma.go.jp/gmd/kaiyou/shindan/index\\_wave.html](https://www.data.jma.go.jp/gmd/kaiyou/shindan/index_wave.html)).

140 Temperature ( $^{\circ}\text{C}$ ), salinity ( $\text{‰}$ ) and turbidity (NTU) were measured *in situ* at the four nearshore  
141 field sites (A1–4, Figure 1) at the same time that water samples were collected. There was a  
142 significant decrease in salinity ( $\sim 15\text{‰}$ ) and concurrent increase of turbidity ( $\sim 10$ -fold) during the  
143 storm on June 16 compared to before the storm on June 13 and afterwards on June 19 (Figure  
144 3). Up to a  $5\text{‰}$  decrease in salinity and 3 NTU increase in turbidity was measured between the  
145 two storms in October (Oct 1 and 3). These changes were smaller in magnitude than were  
146 recorded for the June storm and were not statistically significant, despite the storms in October  
147 delivering much more precipitation than the June storm (Figure 2). However, the wind  
148 accompanying the October storms was also much more intense (Figure 2), which presumably  
149 mixed the water column more thoroughly and prevented freshwater lenses from forming, thus  
150 contributing to diminished changes in salinity and turbidity being observed in October compared  
151 to June.

152 Concentrations of dissolved nutrients—including Nitrate ( $\text{NO}_3^-$ ), Nitrite ( $\text{NO}_2^-$ ), Ammonium  
153 ( $\text{NH}_4^+$ ), Phosphate ( $\text{PO}_4^{3-}$ ), Silica ( $\text{SiO}_2$ ), and dissolved Iron (dFe)—were measured in seawater  
154 samples collected in June and October (Figure 3) and throughout the second mesocosm  
155 experiment (Supplemental Figure 6). Overall, dissolved nutrient concentrations were higher in  
156 June than October, with the exception of dFe and  $\text{SiO}_2$ , which both had similar values in the two  
157 sampling months (Figure 3). A nonparametric Kruskal-Wallis test was applied to detect  
158 significant storm-induced differences in field nutrient concentrations (Supplemental Table 3).  
159 Results showed significant increases ( $p < 0.05$ ) in  $\text{NO}_2^-$  concentrations during and following  
160 storm events in June and October, whereas  $\text{SiO}_2$  and  $\text{PO}_4^{3-}$  were only significantly elevated  
161 during and after the storm in June (Figure 3).

162 Red soil addition in the October mesocosm experiment caused a significant increase in SiO<sub>2</sub>  
163 concentration (Supplemental Figure 6, Supplemental Table 4). Additionally, red soil addition  
164 caused PO<sub>4</sub><sup>3-</sup> concentration to increase above the detection limit 4 hours following soil addition,  
165 whereas the concentration of PO<sub>4</sub><sup>3-</sup> stayed below the detection limit in control mesocosms after  
166 the initial measurement (Supplemental Figure 6). Two-way ANOVA results (Supplemental Table  
167 4) indicate that time had a greater effect on nutrient concentration ( $p < 0.05$  for NO<sub>2</sub><sup>-</sup>, SiO<sub>2</sub> and  
168 dFe) than red soil treatment ( $p < 0.05$  for SiO<sub>2</sub> and dFe). The treatment by time interaction was  
169 only significant in the case of SiO<sub>2</sub> ( $p < 0.05$ ), for which higher concentrations were found in soil-  
170 treated mesocosms.

171

## 172 **Bacterial community responses to storm events and red soil input**

173 Metabarcoding with the bacterial 16S ribosomal RNA gene was performed to evaluate  
174 shifts in bacterial community composition associated with extreme storms in the field and with  
175 sediment input in mesocosms. There was a clear shift in the relative abundances of bacterial  
176 phyla in field samples collected during the June storm compared to before or afterwards.  
177 Several phyla that were also present in soil samples became more abundant in the water  
178 samples collected during the storm—including Acidobacteria, Actinobacteria, Chloroflexi,  
179 Firmicutes, Rokubacteria and Verrucomicrobia—but phyla not detected in soil samples also  
180 became more abundant during the storm, most notably Epsilonbacteraeota (Figure 4). Principal  
181 component analysis (PCA) of Aitchison distances between bacterial community compositions in  
182 water samples also clearly illustrated a shift in community composition during the June storm;  
183 samples collected during the storm separated along the primary axis (PC1) from the samples  
184 collected both before and afterwards (Figure 5). The shift in community composition during the  
185 storm was accompanied by an increase in ASV richness (Amplicon Sequence Variants; Figure



186 6); estimated ASV richness was significantly higher in samples collected during the June storm  
187 compared to samples collected before and afterwards.

188         Soil addition to June mesocosms also influenced bacterial community composition and  
189 richness, although to a lesser extent than the storm-influenced nearshore communities.  
190 Bacterial phyla dominant in soil samples were detectable in mesocosm samples taken one hour  
191 after soil addition, but their relative abundance diminished in samples taken 24 hours later  
192 (Figure 4). Likewise, ASV richness increased in samples taken from mesocosms following soil  
193 addition and decreased over time (Supplemental Figure 8). Overall, mesocosm incubation time  
194 had a larger effect on bacterial community composition than soil addition (Figure 4,  
195 Supplemental Figure 9), despite mesocosm conditions (temperature, salinity, dissolved oxygen)  
196 remaining similar to ambient conditions throughout the experiment (Supplemental Figures 4–5).

197         In October, the community composition also shifted between the two storms (Trami and  
198 Kong-Rey) relative to before and after the overall event window. Additionally, some phyla  
199 present in soil samples, particularly Firmicutes, increased in relative abundance within the event  
200 window, but similar to in June, phyla undetected in soil samples also increased in relative  
201 abundance (e.g. Epsilonbacteraeota and Fusobacteria). However, unlike in June,  
202 Actinobacteria, Planctomycetes, and Verrucomicrobia were already detectable in water samples  
203 collected before Typhoon Trami affected Okinawa (Figure 4). PCA further demonstrated a shift  
204 in community composition in samples collected between the October storms compared to  
205 before and afterward; samples collected between the two storms separated on the primary axis  
206 from samples collected before and after the storms (Figure 5). Interestingly, the estimated ASV  
207 richness was lower (by about half) for all samples collected in October compared to in June,  
208 including in soil samples, and estimated richness did not increase in the samples collected  
209 between storms (Figure 6). Community compositions in field samples from the different months  
210 segregated along the primary axis in PCA and the differences were statistically significant using  
211 PERMANOVA ( $p < 0.01$ ,  $F = 5.37$ ,  $R^2 = 0.17$ ), demonstrating that nearshore bacterial

212 communities were distinct in June and October (Supplemental Figure 7). Furthermore, soil  
213 addition to October mesocosms did not cause observable increases in relative abundances of  
214 phyla found in soil samples as it had in June (Figure 4, Supplemental Figure 8).

215 In order to identify individual taxa that became more abundant during storms and, thus,  
216 contributed to the broader patterns observed in the data, we performed pairwise testing for  
217 differentially abundant ASVs between sampling dates in each month. The greatest number of  
218 significantly differentially abundant ASVs were found in the pairwise test between June 13  
219 (before the storm) and June 16 (during the storm), with the vast majority being more abundant  
220 during the storm (Figure 7A). In contrast, very few ASVs were significantly differentially  
221 abundant in samples collected before and after the June storm (Figure 7A). While many of the  
222 ASVs that had significantly higher relative abundance during the storm on June 16 were also  
223 detected in soil samples, the majority were not (Figure 7A, B). ASVs that had significantly higher  
224 relative abundance on June 16 compared to June 13 belonged to a total of 67 orders—including  
225 Flavobacteriales, Campylobacterales, and Vibrionales, which can be pathogenic to humans and  
226 marine organisms (Pruzzo *et al.*, 2005; Silva *et al.*, 2011; Loch and Faisal, 2015; Canty *et al.*,  
227 2020), and Rhizobiales, Sphingomonadales, and Alteromonadales, which were also found in  
228 soil samples (Figure 7B). In pairwise tests for October samples, the largest number of  
229 differentially abundant ASVs were likewise found between samples collected before (Sept. 28)  
230 and between storms (Oct. 1 and 3), but none of the differentially abundant ASVs were also  
231 found in soil samples (Figure 7C, D). ASVs showing significant differences in relative  
232 abundance between samples taken before and between the October storms belonged to 21  
233 different orders, with most, but not all, also represented in the June results (Figure 7D).

234

## 235 **Discussion**

236

237 As the severity and frequency of extreme storm events increases with global climate change, it  
238 is increasingly important to understand how these events impact ecological functioning in  
239 marine ecosystems (Wetz and Paerl, 2008; Du *et al.*, 2019). However, characterizing the effects  
240 of extreme storm events, such as typhoons, on coastal ecosystems is a complicated task, due  
241 both to forecast unpredictability, which makes sampling before and after events challenging,  
242 and the dangerous conditions that accompany storms (Chen *et al.*, 2018). This study reports on  
243 the nearshore microbial community dynamics and relevant environmental parameters during  
244 two short sampling campaigns encompassing major storms of the 2018 typhoon season in  
245 Okinawa, Japan. In addition, concurrent, controlled mesocosm experiments were performed to  
246 supplement field observations and isolate impacts of terrestrial sediment input that regularly  
247 accompanies large storms in Okinawa. Predictably, storms caused influxes of both freshwater  
248 and sediment into the coastal marine environment (Figure 3, Supplemental Figure 1), which  
249 carried some soil-derived bacteria and some bacteria presumably derived from other terrestrial  
250 sources (e.g. urban or agricultural wastewater; Figures 4 and 7). The storm effects were short-  
251 lived, however, and bacterial community compositions in samples collected before and after  
252 storms were largely similar (Figures 4, 5, 7). While field samples were collected three days after  
253 storm events, mesocosm experiments showed that bacteria introduced with soil additions  
254 diminished in relative abundance just four hours after soil input and were no longer detectable  
255 24 hours later. Despite the rapidity of community shifts, terrestrially derived bacteria and marine  
256 bacteria that increased in relative abundance during and after storms may still influence coastal  
257 biogeochemical cycling and, in some cases, could be detrimental to the coastal ecosystem or  
258 dangerous to human health. For instance, Rhodobacteraceae bacteria (order Rhodobacterales),  
259 which became relatively more abundant during storms (Figure 7), are known to rapidly and  
260 competitively exploit transient sources of particulate and dissolved organic matter and thus may  
261 enhance remineralization in nearshore waters (Buchan *et al.*, 2014). Other bacteria that  
262 increased in relative abundance during and after storms can cause diseases in reef-building

263 corals (e.g. *Vibrio spp.*, *Pseudoalteromonas sp.*) and humans (e.g. *Campylobacter*,  
264 *Fusobacteria*, *Enterobacter*) (Pruzzo *et al.*, 2005; Vizcaino *et al.*, 2010; Silva *et al.*, 2011;  
265 Zimmer *et al.*, 2014); Figure 7, Supplemental Tables 6 and 7), emphasizing the need to better  
266 understand sources and sinks of these bacteria in the coastal environment.

267

268 **Extreme storms cause rapid changes in environmental conditions and bacterial**  
269 **community composition**

270

271 During the storm event in June, we measured decreased salinity and increased turbidity in  
272 nearshore surface waters (Figure 3), which is similar to previous reports following major storm  
273 events (De Carlo *et al.*, 2007; Zhou *et al.*, 2012; Chen *et al.*, 2018). Freshwater and sediment  
274 input was accompanied by moderate increases in  $\text{NO}_2^-$ ,  $\text{NO}_3^-$ ,  $\text{NH}_4^+$ ,  $\text{PO}_4^{3-}$ ,  $\text{SiO}_2$  and dFe  
275 concentrations that ranged from a few nM, in the case of dFe, to up to 25  $\mu\text{M}$  for  $\text{SiO}_2$  (Figure 3)  
276 and is consistent with terrestrial run-off from agricultural areas with high iron-content soil, as is  
277 found in Okinawa (Arakaki *et al.*, 2005). However, nutrient loading dissipated before samples  
278 were collected again three days after the June storm (Figure 3). Bacterial diversity (ASV  
279 richness, Figure 6) increased during the storm, representing the introduction of bacterial taxa  
280 that were also found in our soil samples and are common components of soil microbiomes,  
281 including Acidobacteria, Actinobacteria, Chloroflexi, Firmicutes, Planctomycetes, Rokubacteria  
282 and Verrucomicrobia (Figure 4; Freitas *et al.*, 2012; Witt *et al.*, 2012; Balmonte *et al.*, 2016; Lin  
283 *et al.*, 2019). Many of these taxa are also commonly associated with particulate matter in marine  
284 environments (e.g. Planctomycetes, Actinobacteria, and Verrucomicrobia) making resuspension  
285 of marine sediment during storms another potential contributing source of these bacteria  
286 (DeLong *et al.*, 1993; Crespo *et al.*, 2013). *Campylobacteriales* (Epsilonbacteraeota) that  
287 increased in relative abundance during storms could also derive from agricultural waste being  
288 incorporated into run-off (Jones, 2001).

289

290 Three days after the storm, on June 19, the bacterial diversity returned to pre-storm levels  
291 (Figure 6A) and the community composition was almost identical to before the storm (Figure  
292 5A). Moreover, only 19 ASVs were significantly differentially abundant between June 13 and  
293 June 19 compared to 267 ASVs between June 13 and June 16 (Figure 7A), demonstrating the  
294 high speed at which the microbial community recovered. This high speed largely contrasts with  
295 previous field studies where longer periods of time (i.e. from weeks to months) were needed to  
296 restore pre-storm microbial compositions (De Carlo *et al.*, 2007; Yeo *et al.*, 2013). The  
297 ephemerality of terrestrially-derived bacteria after introduction to the coastal environment was  
298 similarly apparent in results from the June mesocosm experiment. We detected phyla dominant  
299 in soil samples (e.g. Acidobacteria, Chloroflexi, Firmicutes, and Planctomycetes) in treatment  
300 mesocosms one hour after soil was added, but the relative abundances of these phyla  
301 decreased in samples taken four and twelve hours later, and they were no longer detectable in  
302 samples taken 24 hours later. The transience of storm-effects on nearshore bacterial  
303 communities was further demonstrated in results from the October storm event. The bacterial  
304 community recovered just three days after super-typhoon Kong-Rey passed, the second super-  
305 typhoon to affect Okinawa in less than a week (Figure 5B). This transience may, in part, reflect  
306 terrestrial and freshwater bacteria lysing in seawater due to osmotic stress. However, enteric  
307 bacteria are able to survive in seawater, particularly when organic material is readily available  
308 (Munro *et al.*, 1989). Settling was likely also a contributing factor, as many of the bacterial taxa  
309 that increased in relative abundance during storms and after soil addition to mesocosms are  
310 known to associate with sediment surfaces (DeLong *et al.*, 1993; Duret *et al.*, 2019) and some  
311 sedimentation was visible in mesocosm bottles despite using pumps to maintain water  
312 circulation. Moreover, tidal flushing may have transported introduced or resuspended bacteria  
313 offshore.

314

315 **Extreme storms cause context-dependent changes in environmental conditions and**  
316 **bacterial community composition**

317

318 While storm effects were transient in both cases (Figure 5), the June and October storm  
319 events affected coastal physicochemistry and bacterial community composition differently  
320 (Figures 3, 4). Events in both June and October increased coastal nitrogen loading, but only the  
321 June event was accompanied by increased  $\text{PO}_4^{3-}$  and  $\text{SiO}_2$  concentrations, and the June storm  
322 caused more pronounced shifts in bacterial community composition, highlighted by a larger  
323 increase in ASV richness and a higher number of differentially abundant ASVs (Figure 7).  
324 Although these differences in both nutrient loading and bacterial communities, may reflect  
325 disparate sampling schemes, it is likely that differences in rain and wind intensity, as well as the  
326 contexts in which the two events occurred, had strong effects. It has been shown that wind  
327 speed alone can drive alpha diversity shifts in epipelagic bacterial communities (Bryant *et al.*,  
328 2016). Key differences between the June and October events were that much more rain, wind  
329 and wave action accompanied the October storm event than the June storm and that the June  
330 storm made landfall at the beginning of the typhoon season, whereas the October storms  
331 affected Okinawa towards the end of the typhoon season.

332 Typhoon Trami, on Sept. 29, caused twice as much precipitation as tropical storm  
333 Gaemi, on June 16 (Figure 2), which could have diluted nutrient loading in storm run-off and  
334 caused the smaller changes in nutrient concentrations recorded in October compared to in June  
335 (Figure 3). When flushing rate is high, less  $\text{PO}_4^{3-}$  is desorbed from sediments and there is a  
336 dilution effect for both dissolved phosphorus and nitrogen in run-off (Blanco *et al.*, 2010).  
337 Additionally, Gaemi was the first major storm of the 2018 typhoon season (June–October)  
338 following a relatively prolonged dry period, which could increase nutrient loading in storm run-  
339 off, especially since agricultural fertilizers are applied throughout the preceding spring and  
340 summer growing season. By October, several tropical storms and typhoons had already

341 affected Okinawa (Figure 2); the 2018 Pacific typhoon season had higher than average storm  
342 frequency and included 29 tropical storms, 13 typhoons, and 7 super typhoons, although not all  
343 made direct landfall with Okinawa (Japan Meteorological Agency,  
344 <https://www.jma.go.jp/jma/indexe.html>). These intervening events could strip topsoil and deplete  
345 soil nutrients and microbiomes, so that October storm run-off carried less nutrients, organic  
346 material, and terrestrial bacteria into coastal water than storm run-off in June. Moreover,  
347 antecedent soil moisture affects dissolved nutrient loading in run-off, with less nutrients  
348 desorbing from clay-based soils, like Okinawa red soil, when already wet (Perrone and  
349 Madramootoo, 1998).

350         The controlled mesocosm experiments offer additional insight for interpreting differences  
351 in field observations between June and October. Despite collecting soil from the same place in  
352 June and October, the soil microbiome in October had half the bacterial richness as in June  
353 (Figure 6) and soil addition to October mesocosms did not introduce soil bacteria or increase  
354 bacterial richness as it had in June mesocosms (Figure 4, Supplemental Figure 9). These  
355 results suggest that run-off from storms occurring towards the end of the typhoon season may  
356 carry less diverse bacterial assemblages than run-off from early-season storms. Furthermore,  
357 soil addition in October mesocosms did not cause nitrogen ( $\text{NO}_2^-$  or  $\text{NO}_3^-$ ) or dFe to increase  
358 over baseline measurements, but did cause increases in  $\text{SiO}_2$  and  $\text{PO}_4^{3-}$  (Supplemental Figure  
359 6). However, the increase in  $\text{SiO}_2$  and  $\text{PO}_4^{3-}$  were gradual, demonstrating that time is required to  
360 release these compounds from red soil (De Carlo *et al.*, 2007; Blanco *et al.*, 2010; Chen *et al.*,  
361 2018). Soils in Okinawa could, therefore, have lower nitrogen content at the end of the typhoon  
362 season and more intense rains may deliver less nutrients due to rapid flushing.

363

#### 364 **Influence of extreme storms on bacterial taxa in nearshore waters**

365

366 The influence of June and October storms on coastal microbial communities varied in effect  
367 size, but in both instances the community shift was rapid and transient and included shared  
368 bacterial groups that became more abundant during and after storms in both months; 15 out of  
369 the 21 bacterial orders encompassing ASVs that were significantly more abundant during the  
370 October event were shared with the June event (Figure 7). The shared bacterial orders included  
371 primarily heterotrophic bacteria, several of which contain potentially pathogenic groups (e.g.  
372 Vibrionales, Fusobacteriales, and Campylobacterales) ([Pruzzo et al. 2005](#); [Silva et al. 2011](#);  
373 [Canty et al. 2020](#)). Originally, we expected cyanobacteria to respond to increased inorganic  
374 nutrients delivered to the coastal ecosystem with storm run-off. Specifically, we expected  
375 nitrogen fixers—such as *Trichodesmium*, which occasionally blooms near Okinawa (Grossmann  
376 *et al.*, 2015)—to benefit from increased dFe and  $\text{PO}_4^{3-}$  in run-off (Sañudo-Wilhelmy *et al.*, 2001;  
377 Wu *et al.*, 2003). Instead, only a few cyanobacteria ASVs became more abundant during the  
378 June storm, but not the October storm (Figure 7). Namely, cyanobacteria belonging to the family  
379 Oscillatoriaceae, which form filamentous benthic mats (Siegesmund *et al.*, 2008; Engene *et al.*,  
380 2018), and Obscuribacterales, which are uncultured and have unknown morphology, but may  
381 not be photosynthetic (Soo *et al.*, 2014), became more abundant in June.

382 There are several possible explanations for the minimal changes in cyanobacteria relative  
383 abundance: i) cyanobacteria were not limited by compounds present in run-off, ii) nutrients in  
384 run-off were not biologically available, or iii) terrestrial run-off was transported offshore or diluted  
385 too quickly to affect nearshore communities. Nutrient concentrations that were elevated during  
386 the June storm ( $\text{NO}_2^-$ ,  $\text{NO}_3^-$ ,  $\text{PO}_4^{3-}$  and dFe) decreased after the storm passed, but not  
387 immediately and not as quickly as microbial communities recovered (Figures 3, 4). Since these  
388 nutrients were not immediately drawn down, the photosynthetic microbial community may not  
389 have been nutrient limited in our study area. That microbial communities did not respond to soil  
390 addition in mesocosms, despite increased  $\text{PO}_4^{3-}$  and dFe, further suggests that nutrient  
391 availability was not driving major changes in bacterial community composition.



392 Heterotrophic bacteria increasing in relative abundance during and after storms could derive  
393 from soil or other components of run-off, have been resuspended from the seafloor due to wind  
394 and waves, or have responded to increased organic matter from run-off. These bacteria may  
395 affect ecosystem functioning by remineralizing organic matter within the near-shore environment  
396 (Buchan et al. 2014; Kieft et al. 2018) or by causing opportunistic infections in keystone  
397 metazoans (Pruzzo et al. 2005; Silva et al. 2011; Canty et al. 2020), thus making it important to  
398 identify their source. Rare bacteria often become more abundant during or after disturbances  
399 (Preisner et al. 2016; Fuentes et al. 2016; Sjöstedt et al. 2012), but it is difficult to parse out their  
400 sources (Shade et al. 2014). Such conditionally rare bacteria may result from introductions or  
401 opportunistic growth of previously undetectable bacteria (Shade et al. 2014). Discriminating  
402 between these potential sources is challenging with current methods, but prolonged intensive  
403 sampling better resolves the dynamics of rare taxa (Shade et al. 2013; Shade et al. 2014).  
404 Beyond working towards establishing the more long term dynamics of nearshore  
405 bacterioplankton communities, future work aimed at characterizing bacteria in wastewater  
406 outflows and stormwater could also help determine whether bacteria that become more  
407 abundant during storms represent introductions or expansions.

408

#### 409 **Potential ecosystem consequences due to terrestrial run-off from extreme storms**

410

411 Despite being short-lived, the changes we observed in bacterial community composition and  
412 environmental parameters during storms can nevertheless be detrimental to both the coastal  
413 ecosystem and human health. While most terrestrially-derived bacteria are benign to marine  
414 ecosystems, many are potentially pathogenic to corals and other marine organisms (Sutherland  
415 *et al.*, 2004; Haapkylä *et al.*, 2011; Pollock *et al.*, 2014; Sheridan *et al.*, 2014). Terrestrial run-off  
416 has been implicated in coral diseases, such as White Pox Disease and Red Band Disease, in  
417 many tropical and subtropical locations, including Madagascar (Haapkylä *et al.*, 2011; Pollock *et*

418 *al.*, 2014; Sheridan *et al.*, 2014), the Caribbean (Frias-Lopez *et al.*, 2002; Patterson *et al.*,  
419 2002), and Australia's Great Barrier Reef (Pollock *et al.*, 2014). Furthermore, storm events can  
420 cause water-column mixing and sediment resuspension, leading to pathogenic marine bacteria  
421 that usually inhabit the seafloor to become more abundant in the water column (Hassard *et al.*,  
422 2016). Indeed, in our study we found several strains of *Vibrio spp.*, *Pseudoalteromonas sp.*, and  
423 Rhodobacteraceae bacteria specifically associated with coral disease (Sussman *et al.*, 2008;  
424 Sheridan *et al.*, 2014) to be significantly enriched in samples we collected during or following  
425 storm events (Supplemental Table 5). Considering the additional stress caused by turbidity and  
426 sedimentation during storm events, alongside potentially decreased pH and dissolved oxygen  
427 due to enhanced heterotrophic bacterial respiration (Weber *et al.*, 2012; Altieri *et al.*, 2017),  
428 corals and other organisms may be especially susceptible to pathogen infection during and after  
429 extreme storms.

430  
431 Heavy rains and floods have long been implicated in transporting human pathogens (e.g. fecal  
432 coliform bacteria) to the marine environment (Pandey *et al.*, 2014; De Jesus Crespo *et al.*,  
433 2019). Indeed, we found bacterial taxa that are potentially dangerous to humans—including  
434 Campylobacteriales, Fusobacteriales, Bacillales, Clostridiales and Enterobacteriales (Bennett  
435 and Eley, 1993; Sharma *et al.*, 2003; Davin-Regli *et al.*, 2019)—significantly enriched during and  
436 following storms. Many of these bacteria were not detected in soil samples, suggesting  
437 additional sources of bacterial contamination in storm run-off. For instance, some of the  
438 Bacillales and Enterobacteriales ASVs enriched in storm-influenced water samples were not  
439 present in soil samples and none of the enriched Clostridiales, Campylobacteriales and  
440 Fusobacteriales ASVs were also found in soil samples (Figure 7). Likewise, these taxa were not  
441 found in mesocosms following soil addition in June or October, demonstrating the larger effect  
442 of storms and run-off on the coastal ecosystem than simply transporting sediment into the  
443 water. Human pathogens may derive from live-stock, storm drains, or overwhelmed waste

444 treatment plants during storms (Weiskel *et al.*, 1996; Jamieson *et al.*, 2004). Interestingly, these  
445 taxa were already present in water samples collected on September 28—although they were  
446 more abundant on October 1 and 3—further indicating a cumulative effect of the typhoon  
447 season on the coastal ecosystem and emphasizing the context-dependency of storm effects.  
448 Ultimately, swimmers and other recreational users need to be aware that pathogenic bacteria  
449 are likely present in Okinawa coastal waters following large rain events. This is not currently the  
450 case in Okinawa as it is in other locations with more robust coastal monitoring programs in  
451 place (e.g. the Southern California Water Research Project or the DNAqua-Net European  
452 project ).

453

#### 454 **Conclusions & Future Directions**

455

456 Despite challenges associated with sampling marine ecosystems during tropical storms and  
457 typhoons, this study describes the timing and nature of storm effects on coastal bacterial  
458 communities in Okinawa, Japan. We found that storm effects were transient, but highly context-  
459 dependent. We coupled controlled mesocosm studies with field observations in an effort to  
460 disentangle the effects of extreme wind and waves and enhanced currents from the effects of  
461 soil input during storms. While the mesocosm results were useful, future studies would benefit  
462 from more realistic run-off simulation (e.g. Le *et al.*, 2016) than the soil additions we employed.  
463 Furthermore, it remains that we did not perform bacterial cell counts or otherwise measure  
464 bacterial biomass or metabolic activity, thus leaving the possibility that run-off increased  
465 microbial biomass or differentially affected microbial physiology. Future studies may capture  
466 such responses by measuring bacterial respiration rates or by performing metatranscriptomics.

467

468 It is important to note that environmental effects of extreme storms will vary in terms of intensity,  
469 spatial extent and duration in different ecosystems and need to be evaluated locally (Paerl *et al.*,

470 2006; Zhang *et al.*, 2009; Herbeck *et al.*, 2011). Storm effects were transient in the open, tidally-  
471 flushed Okinawa coast, but more prolonged storm effects have been observed in other coastal  
472 systems, particularly semi-enclosed areas, such as bays and estuaries, where terrestrial  
473 sediment loads can have residence times from weeks to years (Paerl *et al.*, 2001; Zhang *et al.*,  
474 2009; Herbeck *et al.*, 2011). Therefore, we suggest that the short-term study of typhoon events  
475 follow an adaptive sampling strategy (Wetz and Paerl, 2008), which involves the definition of  
476 well-established baselines for various physicochemical and biological parameters.

477

478 Finally, the transient nature of storm effects described here should not be viewed as diminishing  
479 their potential impact on reef or human health. Differentially abundant bacteria during storms  
480 may cause disease in marine organisms and humans. With future climate change scenarios  
481 predicting more frequent and destructive storms and continued expansion of tourism and  
482 agriculture activities, it is likely that the amount of terrestrial run-off and associated risks will  
483 escalate in the future. This makes regional monitoring programs, including a comprehensive  
484 understanding of background conditions, essential for better interpretations of ecological  
485 consequences from extreme storm events.

486

487

## 488 **Experimental Procedures**

489

### 490 **Study setting**

491 Seawater was collected for metabarcoding and physicochemical analysis from four nearshore  
492 sampling points approximately 250–500 m apart, along the central west coast of Okinawa  
493 Island—a semi-urban region with mixed land-use, including agriculture and coastal development  
494 projects (Figure 1). The sampling points (A1–4) were each at least 1.2 km from the nearest  
495 concentrated fresh-water input (e.g. streams or rivers). At the start of the 2018 typhoon season,

496 samples were collected before (June 13), during (June 16), and after (June 19) tropical storm  
497 Gaemi, which struck Okinawa on June 16, 2018 and caused a red soil pollution event (Figure 2,  
498 Supplemental Figure 2A). Towards the end of the typhoon season, samples were collected  
499 before (Sept 28), during (Oct 1 and Oct 3) and after (Oct 8) a red soil pollution event caused by  
500 typhoon Trami, which made landfall with Okinawa on September 30, and was prolonged by  
501 Typhoon Kong-Rey, which approached Okinawa on October 5th (Figure 2, Supplemental Figure  
502 2B–C).

503

#### 504 **Seawater sampling for DNA and physicochemical analysis**

505 Surface seawater was collected for DNA metabarcoding by submerging clean 500 mL Nalgene  
506 bottles just below the sea surface. Seawater for dissolved Fe (dFe) and nutrient analysis was  
507 collected in acid-cleaned 50 mL Falcon tubes. Physicochemical properties—dissolved oxygen  
508 (DO), salinity, temperature, and turbidity—were measured with a CTD probe (RINKO, JFE  
509 Advantech, Japan) at each site. After being immediately transported to the laboratory, seawater  
510 samples for metabarcoding were filtered through 0.2 µm pore-size Polytetrafluoroethylene  
511 (PTFE) filters (Millipore) under gentle vacuum and filters were stored at -20 °C for later DNA  
512 extraction. Seawater samples for dFe and nutrient analysis were filtered through 0.45 µm pore-  
513 size acid-washed Teflon digiFILTERS (SPC Science, Canada) and filtered water samples were  
514 stored at -20 °C for later chemical analysis.

515

#### 516 **Mesocosm experimental design**

517 Seawater was collected for concurrent mesocosm experiments on June 11 (26.512 °N,  
518 127.872°E) and October 10 (26.479 °N, 127.829 °E). Nearshore coastal seawater was pumped  
519 from just below the sea surface and filtered through 1 mm and 300 µm nylon mesh screen sizes  
520 to remove debris and larger organisms. Acid-cleaned 22 L clear-plastic carboys were rinsed  
521 twice with 300 µm nylon mesh-size filtered seawater before filling to 20 L with filtered seawater.

522 Bottles were covered with parafilm and kept shaded during transport to the Okinawa Institute of  
523 Science and Technology (OIST) Marine Science Station, where they were submerged in a basin  
524 with continuous flow-through seawater to keep conditions within the bottles similar to natural  
525 conditions. Mesocosm bottles were topped with silicone sponge stoppers to allow gas  
526 exchange, but limit evaporation and prevent dust, water or other contaminants from entering the  
527 bottles during the experiment (Supplemental Figure 3). Small pumps were included in each  
528 mesocosm to maintain water circulation ( $2 \text{ L min}^{-1}$ ). HOBO temperature and light loggers  
529 (Onset) were fastened to the pumps and at the same depth in the basin surrounding  
530 mesocosms to ensure that mesocosms conditions remained similar to ambient conditions  
531 (Supplemental Figure 4). Salinity and DO were measured each time water was sampled from  
532 the mesocosms throughout the experiment (Supplemental Figure 5). Mesocosms experiments  
533 included 9–10 mesocosms: 4–5 control replicates (four in June and five in October) and 5  
534 treatments replicates with red soil added to an ecologically relevant high concentration of  $200$   
535  $\text{mg L}^{-1}$  (O'Connor *et al.*, 2016). Mesocosms were sampled (100 mL for metabarcoding, 50 mL  
536 for dFe and nutrient concentration) with 50 mL sterile pipettes before the experiment started  
537 ( $t_0$ ), and 1, 4, 12, 24, and 48 h following red soil addition to treatment bottles. Water samples  
538 were processed as described in the previous section.

539

#### 540 **Red soil collection for mesocosm experiments and DNA analysis**

541 Soil samples were collected from an open agricultural field with exposed soil ( $26.507^\circ \text{N}$ ,  
542  $127.868^\circ \text{E}$ ), on June 10 and October 9 for addition to red soil treated mesocosms and to  
543 evaluate soil microbiomes. Soil samples were sieved through  $330 \mu\text{m}$  mesh and maintained at  
544  $4^\circ \text{C}$  for 24 h until use in the mesocosm experiment. To determine soil moisture content, 10 g  
545 subsamples ( $n=10$ ) were weighed and dried at  $100^\circ \text{C}$  by following the standard method AS  
546 1289.2.1.1-2005 (Standards Association of Australia). Soil moisture content was used to  
547 calculate how much wet soil should be added to mesocosms in order to reach the final

548 concentration of 200 g soil (dry weight) per L seawater. In both June (n=4) and October (n=2),  
549 additional 50 g aliquots of soil were kept at -20 °C for subsequent metabarcoding analysis.

550

#### 551 **Chemical analysis: dFe and major nutrients**

552 Dissolved Fe (dFe) concentration was determined following the methodology of Wu and Boyle  
553 (1998). This method uses a Mg (OH)<sub>2</sub> co-precipitation to pre-concentrate Fe from seawater  
554 followed by an isotope dilution method. Seawater dFe was quantified using an internal standard  
555 element (<sup>57</sup>Fe) with inductively coupled plasma mass spectrometry (Element 2, Thermo  
556 Scientific). The mass spectrometer was operated in medium-resolution mode with 4000  
557 resolution (FWHM). The mass calibration was performed using a multi-element ICP-MS tune-up  
558 solution (Thermo Fisher Scientific). In order to ensure the quality of the ICP-MS analysis, control  
559 standards and samples (i.e. analytical replicates, certified reference material and analytical  
560 blank) were analyzed once every 12 samples. Recovery of Fe from reference certified material  
561 QC3163 (Sigma-Aldrich, USA) was satisfactory and ranged from 65 to 80%. The overall error  
562 associated with the analytical process was typically lower than 5% and never higher than 15%.  
563 All measurements were above the instrument's detection limit. Analysis was carried out at the  
564 OIST Instrumental Analysis Section mass spectrometry laboratory. Special attention was paid to  
565 avoid Fe contamination and an exhaustive cleaning process was carried out following the  
566 methods of (King and Barbeau, 2011).

567

568 Nutrient concentrations—including Nitrate (NO<sub>3</sub><sup>-</sup>), Nitrite (NO<sub>2</sub><sup>-</sup>), Ammonium (NH<sub>4</sub><sup>+</sup>), Phosphate  
569 (PO<sub>4</sub><sup>3-</sup>) and Silica (SiO<sub>2</sub>)—were determined on a QuAAtro39 Continuous Segmented Flow  
570 Analyzer (SEAL Analytical) following manufacturer guidelines. Final concentrations were  
571 calculated through AACE software (SEAL Analytical). Nutrient Analysis was carried out at the  
572 Okinawa Prefecture Fisheries and Ocean Technology Center.

573

574 **Nutrient and dFe statistical analyses**

575 Mesocosm data were found to be normally distributed with a Shapiro-Wilks test and, therefore,  
576 a one-way ANOVA was performed to test overall differences between treatments. Post-hoc  
577 Tukey HSD analysis was performed to identify which specific groups differed. Field data were  
578 not normally distributed, regardless of transformation, so a Kruskal-Wallis test was used to test  
579 for significant differences between sampling dates. Analyses were performed within the R  
580 statistical environment (R Core Team 2018).

581

582 **DNA extraction and metabarcode sequencing**

583 DNA was extracted from frozen PTFE filters following the manufacturer protocol for the DNeasy  
584 PowerWater Kit (Qiagen), including the optional heating step. DNA was extracted from soil  
585 samples by following manufacturer protocol for the DNeasy PowerSoil Kit (Qiagen).

586 Metabarcode sequencing libraries were prepared for the V3/V4 region of the bacterial 16S  
587 ribosomal RNA gene following Illumina's "16S Metagenomic Sequencing Library Preparation"  
588 manual without any modifications. Sequencing libraries were transferred to the OIST  
589 Sequencing Center for 2x300-bp sequencing on the Illumina MiSeq platform with v3 chemistry.  
590 Overall, 18.4 million sequencing reads were generated in this study, with 76,217–219,584  
591 sequencing reads per sample (mean = 137,585). Sequencing data are available from the NCBI  
592 Sequencing Read Archive under the accession PRJNA564579.

593

594 **Metabarcode analyses**

595 Sequencing reads were denoised using the Divisive Amplicon Denoising Algorithm (Callahan *et al.*  
596 *et al.*, 2016) with the DADA2 plug-in for QIIME 2 (Bolyen *et al.*, 2019). Following denoising, 11.8  
597 million sequences remained with 11,061–153,646 sequences per sample (mean = 88,033). A  
598 total of 36,007 ASVs were identified in our dataset, with 64–2,886 unique ASVs observed per



599 sample (mean = 642). Taxonomy was assigned to representative ASVs using a Naive Bayes  
600 classifier trained on the SILVA 97% consensus taxonomy (version 132, Quast *et al.*, 2013) with  
601 the QIIME 2 feature-classifier plug-in (Bokulich *et al.*, 2018). The results were imported into the  
602 R statistical environment (R Core Team 2018) for further analysis with the Bioconductor  
603 phyloseq package (McMurdie and Holmes, 2013). The ASV richness for each sample was  
604 estimated using the R package breakaway (Willis and Bunge, 2015) and differences in  
605 estimated richness between sample types were tested for with the betta function (Willis *et al.*,  
606 2017). In order to minimize compositional bias inherent in metabarcoding data as much as  
607 possible, we used the Aitchison distance between samples, which includes a centered log ratio  
608 transformation to normalize data (Gloor *et al.*, 2017), for principal component analyses (PCA).  
609 Permutational analyses of variance (PERMANOVA) on Aitchison distances were performed with  
610 the adonis function (999 permutations) in the R package vegan (Oksanen *et al.*, 2019) to test  
611 whether shifts in community composition were statistically significant. Lastly, we used the  
612 DESeq2 bioconductor package (Love *et al.*, 2014) to determine which ASVs were significantly  
613 differentially abundant (False Discovery Rate adjusted  $p$ -value < 0.05) in water samples  
614 collected from field sites before, during, and after storms. We then checked if significantly  
615 differentially abundant ASVs were also present in soil samples from respective months to  
616 assess whether differentially abundant ASVs were soil-derived. Intermediate data files and the  
617 code necessary to replicate analyses are available in a GitHub repository:  
618 <https://github.com/maggimars/RedSoil>.

619

## 620 **Acknowledgments**

621 We thank Akinori Murata and Marine Le Gal for help with sample collection, Kazumi Inoha,  
622 Koichi Toda, Kosuke Mori and Okinawa Marine Science Support Section, OIST for assistance  
623 with experimental design and technical support and Koichi Kinjo from the Okinawa Prefectural

624 Institute of Health and Environment for his advice. We also thank OIST sequencing center for  
625 DNA sequence support and Okinawa Prefecture Fisheries and Ocean Technology Center for  
626 nutrient analysis assistance. MMB was supported by a Japan Society for the Promotion of  
627 Science (JSPS) DC1 graduate student fellowship. This work was supported by the JSPS  
628 KAKENHI program [Early-Career Project No. 18K18203] and the OIST Marine Biophysics Unit.  
629 Furthermore, we confirm that we have no conflicts of interest to disclose.

630

631

## 632 Reference list

- 633 Altieri, A.H., Harrison, S.B., Seemann, J., Collin, R., Diaz, R.J., and Knowlton, N. (2017)  
634 Tropical dead zones and mass mortalities on coral reefs. *Proc Natl Acad Sci U S A* **114**:  
635 3660–3665.
- 636 Anderson, T.H. and Taylor, G.T. (2001) Nutrient pulses, plankton blooms, and seasonal hypoxia  
637 in western Long Island Sound. *Estuaries* **24**: 228–243.
- 638 Arakaki, T., Fujimura, H., Hamdun, A.M., Okada, K., Kondo, H., Oomori, T., et al. (2005)  
639 Simultaneous Measurement of Hydrogen Peroxide and Fe Species (Fe(II) and Fe(tot)) in  
640 Okinawa Island Seawater: Impacts of Red Soil Pollution. *J Oceanogr* **61**: 561–568.
- 641 Azam, F., Fenchel, T., Field, J.G., Gray, J.S., Meyer-Reil, L.A., and Thingstad, F. (1983) The  
642 Ecological Role of Water-Column Microbes in the Sea. *Marine Ecology Progress Series* **10**:  
643 257–263.
- 644 Balmonte, J.P., Arnosti, C., Underwood, S., McKee, B.A., and Teske, A. (2016) Riverine  
645 Bacterial Communities Reveal Environmental Disturbance Signatures within the  
646 Betaproteobacteria and Verrucomicrobia. *Front Microbiol* **7**: 1441.
- 647 Bennett, K.W. and Eley, A. (1993) Fusobacteria: new taxonomy and related diseases. *J Med*  
648 *Microbiol* **39**: 246–254.
- 649 Blanco, A.C., Nadaoka, K., and Yamamoto, T. (2008) Planktonic and benthic microalgal  
650 community composition as indicators of terrestrial influence on a fringing reef in Ishigaki  
651 Island, Southwest Japan. *Mar Environ Res* **66**: 520–535.
- 652 Blanco, A.C., Nadaoka, K., Yamamoto, T., and Kinjo, K. (2010) Dynamic evolution of nutrient  
653 discharge under stormflow and baseflow conditions in a coastal agricultural watershed in  
654 Ishigaki Island, Okinawa, Japan. *Hydrol Process* **24**: 2601–2616.
- 655 Bokulich, N.A., Kaehler, B.D., Rideout, J.R., Dillon, M., Bolyen, E., Knight, R., et al. (2018)  
656 Optimizing taxonomic classification of marker-gene amplicon sequences with QIIME 2's q2-  
657 feature-classifier plugin. *Microbiome* **6**: 90.
- 658 Bolyen, E., Rideout, J.R., Dillon, M.R., Bokulich, N.A., Abnet, C.C., Al-Ghalith, G.A., et al.  
659 (2019) Reproducible, interactive, scalable and extensible microbiome data science using  
660 QIIME 2. *Nat Biotechnol* **37**: 852–857.
- 661 Brodie, J.E., Kroon, F.J., Schaffelke, B., Wolanski, E.C., Lewis, S.E., Devlin, M.J., et al. (2012)  
662 Terrestrial pollutant runoff to the Great Barrier Reef: An update of issues, priorities and  
663 management responses. *Mar Pollut Bull* **65**: 81–100.
- 664 Bryant, J.A., Aylward, F.O., Eppley, J.M., Karl, D.M., Church, M.J., and DeLong, E.F. (2016)  
665 Wind and sunlight shape microbial diversity in surface waters of the North Pacific

666 Subtropical Gyre. *ISME J* **10**: 1308–1322.

667 Buchan, A., LeClerc, G.R., Gulvik, C.A., and González, J.M. (2014) Master recyclers: features  
668 and functions of bacteria associated with phytoplankton blooms. *Nat Rev Microbiol* **12**:  
669 686–698.

670 Callahan, B.J., McMurdie, P.J., Rosen, M.J., Han, A.W., Johnson, A.J.A., and Holmes, S.P.  
671 (2016) DADA2: High-resolution sample inference from Illumina amplicon data. *Nat Methods*  
672 **13**: 581–583.

673 Canty, R., Blackwood, D., Noble, R., and Froelich, B. (2020) A comparison between farmed  
674 oysters using floating cages and oysters grown on-bottom reveals more potentially human  
675 pathogenic *Vibrio* in the on-bottom oysters. *Environ Microbiol*.

676 Chen, N., Krom, M.D., Wu, Y., Yu, D., and Hong, H. (2018) Storm induced estuarine turbidity  
677 maxima and controls on nutrient fluxes across river-estuary-coast continuum. *Sci Total*  
678 *Environ* **628-629**: 1108–1120.

679 Chen, N., Wu, J., and Hong, H. (2012) Effect of storm events on riverine nitrogen dynamics in a  
680 subtropical watershed, southeastern China. *Sci Total Environ* **431**: 357–365.

681 Crespo, B.G., Pommier, T., Fernández-Gómez, B., and Pedrós-Alió, C. (2013) Taxonomic  
682 composition of the particle-attached and free-living bacterial assemblages in the Northwest  
683 Mediterranean Sea analyzed by pyrosequencing of the 16S rRNA. *Microbiologyopen* **2**:  
684 541–552.

685 Davin-Regli, A., Lavigne, J.-P., and Pagès, J.-M. (2019) *Enterobacter* spp.: Update on  
686 Taxonomy, Clinical Aspects, and Emerging Antimicrobial Resistance. *Clin Microbiol Rev*  
687 **32**:

688 De Carlo, E.H., Hoover, D.J., Young, C.W., Hoover, R.S., and Mackenzie, F.T. (2007) Impact of  
689 storm runoff from tropical watersheds on coastal water quality and productivity. *Appl*  
690 *Geochem* **22**: 1777–1797.

691 De Jesus Crespo, R., Wu, J., Myer, M., Yee, S., and Fulford, R. (2019) Flood protection  
692 ecosystem services in the coast of Puerto Rico: Associations between extreme weather,  
693 flood hazard mitigation and gastrointestinal illness. *Sci Total Environ* **676**: 343–355.

694 DeLong, E.F., Franks, D.G., and Alldredge, A.L. (1993) Phylogenetic diversity of aggregate-  
695 attached vs. free-living marine bacterial assemblages. *Limnol Oceanogr* **38**: 924–934.

696 Du, J., Park, K., Dellapenna, T.M., and Clay, J.M. (2019) Dramatic hydrodynamic and  
697 sedimentary responses in Galveston Bay and adjacent inner shelf to Hurricane Harvey. *Sci*  
698 *Total Environ* **653**: 554–564.

699 Duret, M.T., Lampitt, R.S., and Lam, P. (2019) Prokaryotic niche partitioning between  
700 suspended and sinking marine particles. *Environ Microbiol Rep* **11**: 386–400.

701 Engene, N., Tronholm, A., and Paul, V.J. (2018) Uncovering cryptic diversity of Lyngbya: the  
702 new tropical marine cyanobacterial genus *Dapis* (Oscillatoriales). *J Phycol* **54**: 435–446.

703 Fabricius, K.E. (2005) Effects of terrestrial runoff on the ecology of corals and coral reefs:  
704 review and synthesis. *Mar Pollut Bull* **50**: 125–146.

705 Freitas, S., Hatosy, S., Fuhrman, J.A., Huse, S.M., Welch, D.B.M., Sogin, M.L., and Martiny,  
706 A.C. (2012) Global distribution and diversity of marine Verrucomicrobia. *ISME J* **6**: 1499–  
707 1505.

708 Frias-Lopez, J., Zerkle, A.L., Bonheyo, G.T., and Fouke, B.W. (2002) Partitioning of bacterial  
709 communities between seawater and healthy, black band diseased, and dead coral  
710 surfaces. *Appl Environ Microbiol* **68**: 2214–2228.

711 Fuhrman, J.A., Cram, J.A., and Needham, D.M. (2015) Marine microbial community dynamics  
712 and their ecological interpretation. *Nat Rev Microbiol* **13**: 133–146.

713 Gao, Y., Zhu, B., Yu, G., Chen, W., He, N., Wang, T., and Miao, C. (2014) Coupled effects of  
714 biogeochemical and hydrological processes on C, N, and P export during extreme rainfall  
715 events in a purple soil watershed in southwestern China. *J Hydrol* **511**: 692–702.

716 Glasl, B., Webster, N.S., and Bourne, D.G. (2017) Microbial indicators as a diagnostic tool for

717 assessing water quality and climate stress in coral reef ecosystems. *Mar Biol* **164**: 91.  
718 Gloor, G.B., Macklaim, J.M., Pawlowsky-Glahn, V., and Egozcue, J.J. (2017) Microbiome  
719 Datasets Are Compositional: And This Is Not Optional. *Front Microbiol* **8**:  
720 Groisman, P.Y., Knight, R.W., Easterling, D.R., Karl, T.R., Hegerl, G.C., and Razuvaev, V.N.  
721 (2005) Trends in Intense Precipitation in the Climate Record. *J Clim* **18**: 1326–1350.  
722 Grossmann, M.M., Gallagher, S.M., and Mitarai, S. (2015) Continuous monitoring of near-bottom  
723 mesoplankton communities in the East China Sea during a series of typhoons. *J Oceanogr*  
724 **71**: 115–124.  
725 Haapkylä, J., Unsworth, R.K.F., Flavell, M., Bourne, D.G., Schaffelke, B., and Willis, B.L. (2011)  
726 Seasonal Rainfall and Runoff Promote Coral Disease on an Inshore Reef. *PLoS One* **6**:  
727 e16893.  
728 Harii, S., Hongo, C., Ishihara, M., Ide, Y., and Kayanne, H. (2014) Impacts of multiple  
729 disturbances on coral communities at Ishigaki Island, Okinawa, Japan, during a 15 year  
730 survey. *Mar Ecol Prog Ser* **509**: 171–180.  
731 Hassard, F., Gwyther, C.L., Farkas, K., Andrews, A., Jones, V., Cox, B., et al. (2016)  
732 Abundance and Distribution of Enteric Bacteria and Viruses in Coastal and Estuarine  
733 Sediments-a Review. *Front Microbiol* **7**: 1692.  
734 Hennessy, K.J., Gregory, J.M., and Mitchell, J.F.B. (1997) Changes in daily precipitation under  
735 enhanced greenhouse conditions. *Clim Dyn* **13**: 667–680.  
736 Herbeck, L.S., Unger, D., Krumme, U., Liu, S.M., and Jennerjahn, T.C. (2011) Typhoon-induced  
737 precipitation impact on nutrient and suspended matter dynamics of a tropical estuary  
738 affected by human activities in Hainan, China. *Estuar Coast Shelf Sci* **93**: 375–388.  
739 Hongo, C. and Yamano, H. (2013) Species-Specific Responses of Corals to Bleaching Events  
740 on Anthropogenically Turbid Reefs on Okinawa Island, Japan, over a 15-year Period  
741 (1995–2009). *PLoS One* **8**: e60952.  
742 Inoue, M., Ishikawa, D., Miyaji, T., Yamazaki, A., Suzuki, A., Yamano, H., et al. (2014)  
743 Evaluation of Mn and Fe in coral skeletons (*Porites* spp.) as proxies for sediment loading  
744 and reconstruction of 50 yrs of land use on Ishigaki Island, Japan. *Coral Reefs* **33**: 363–  
745 373.  
746 Jamieson, R., Gordon, R., Joy, D., and Lee, H. (2004) Assessing microbial pollution of rural  
747 surface waters: A review of current watershed scale modeling approaches. *Agric Water*  
748 *Manage* **70**: 1–17.  
749 Jones, K. (2001) Campylobacters in water, sewage and the environment. *Symp Ser Soc Appl*  
750 *Microbiol* 68S–79S.  
751 King, A.L. and Barbeau, K.A. (2011) Dissolved iron and macronutrient distributions in the  
752 southern California Current System. *J Geophys Res* **116**: 349.  
753 Le, H.T., Ho, C.T., Trinh, Q.H., Trinh, D.A., Luu, M.T.N., Tran, H.S., et al. (2016) Responses of  
754 Aquatic Bacteria to Terrestrial Runoff: Effects on Community Structure and Key Taxonomic  
755 Groups. *Front Microbiol* **7**: 889.  
756 Lewis, S.E., Schaffelke, B., Shaw, M., Bainbridge, Z.T., Rohde, K.W., Kennedy, K., et al. (2012)  
757 Assessing the additive risks of PSII herbicide exposure to the Great Barrier Reef. *Mar*  
758 *Pollut Bull* **65**: 280–291.  
759 Lin, Y.-T., Lin, Y.-F., Tsai, I.J., Chang, E.-H., Jien, S.-H., Lin, Y.-J., and Chiu, C.-Y. (2019)  
760 Structure and Diversity of Soil Bacterial Communities in Offshore Islands. *Sci Rep* **9**: 4689.  
761 Loch, T.P. and Faisal, M. (2015) Emerging flavobacterial infections in fish: A review. *J Advert*  
762 *Res* **6**: 283–300.  
763 Love, M.I., Huber, W., and Anders, S. (2014) Moderated estimation of fold change and  
764 dispersion for RNA-seq data with DESeq2. *Genome Biol* **15**: 550.  
765 Masucci, G.D. and Reimer, J.D. (2019) Expanding walls and shrinking beaches: loss of natural  
766 coastline in Okinawa Island, Japan. *PeerJ* **7**: e7520.  
767 McMurdie, P.J. and Holmes, S. (2013) phyloseq: an R package for reproducible interactive

768 analysis and graphics of microbiome census data. *PLoS One* **8**: e61217.

769 Mei, W. and Xie, S.-P. (2016) Intensification of landfalling typhoons over the northwest Pacific  
770 since the late 1970s. *Nat Geosci* **9**: 753.

771 Mistri, M., Pitacco, V., Granata, T., Moruzzi, L., and Munari, C. (2019) When the levee breaks:  
772 Effects of flood on offshore water contamination and benthic community in the  
773 Mediterranean (Ionian Sea). *Mar Pollut Bull* **140**: 588–596.

774 Munro, P.M., Gauthier, M.J., Breittmayer, V.A., and Bongiovanni, J. (1989) Influence of  
775 osmoregulation processes on starvation survival of *Escherichia coli* in seawater. *Appl*  
776 *Environ Microbiol* **55**: 2017–2024.

777 O'Connor, J.J., Lecchini, D., Beck, H.J., Cadiou, G., Lecellier, G., Booth, D.J., and Nakamura,  
778 Y. (2016) Sediment pollution impacts sensory ability and performance of settling coral-reef  
779 fish. *Oecologia* **180**: 11–21.

780 Oksanen, J., Guillaume Blanchet, F., Friendly, M., Kindt, R., Legendre, P., McGlinn, D., et al.  
781 (2019) *vegan: Community Ecology Package*. R package version 2.5-4.

782 Omija, T. (2004) Terrestrial inflow of soils and nutrients. *Coral Reefs of Japan* **47**: 64–68.

783 Omori, M. (2011) Degradation and restoration of coral reefs: Experience in Okinawa, Japan.  
784 *Mar Biol Res* **7**: 3–12.

785 Paerl, H.W., Bales, J.D., Ausley, L.W., Buzzelli, C.P., Crowder, L.B., Eby, L.A., et al. (2001)  
786 Ecosystem impacts of three sequential hurricanes (Dennis, Floyd, and Irene) on the United  
787 States' largest lagoonal estuary, Pamlico Sound, NC. *Proc Natl Acad Sci U S A* **98**: 5655–  
788 5660.

789 Paerl, H.W., Crosswell, J.R., Van Dam, B., Hall, N.S., Rossignol, K.L., Osburn, C.L., et al.  
790 (2018) Two decades of tropical cyclone impacts on North Carolina's estuarine carbon,  
791 nutrient and phytoplankton dynamics: implications for biogeochemical cycling and water  
792 quality in a stormier world. *Biogeochemistry* **141**: 307–332.

793 Paerl, H.W., Valdes, L.M., Joyner, A.R., Peierls, B.L., Piehler, M.F., Riggs, S.R., et al. (2006)  
794 Ecological response to hurricane events in the Pamlico Sound system, North Carolina, and  
795 implications for assessment and management in a regime of increased frequency.  
796 *Estuaries Coasts* **29**: 1033–1045.

797 Pandey, P.K., Kass, P.H., Soupir, M.L., Biswas, S., and Singh, V.P. (2014) Contamination of  
798 water resources by pathogenic bacteria. *AMB Express* **4**: 51.

799 Patterson, K.L., Porter, J.W., Ritchie, K.B., Polson, S.W., Mueller, E., Peters, E.C., et al. (2002)  
800 The etiology of white pox, a lethal disease of the Caribbean elkhorn coral, *Acropora*  
801 *palmata*. *Proc Natl Acad Sci U S A* **99**: 8725–8730.

802 Pearman, J.K., Afandi, F., Hong, P., and Carvalho, S. (2018) Plankton community assessment  
803 in anthropogenic-impacted oligotrophic coastal regions. *Environ Sci Pollut Res Int* **25**:  
804 31017–31030.

805 Perrone, J. and Madramootoo, C.A. (1998) Improved curve number selection for runoff  
806 prediction. *Can J Civ Eng* **25**: 728–734.

807 Peters, E.C. (2015) Diseases of Coral Reef Organisms. In *Coral Reefs in the Anthropocene*.  
808 Birkeland, C. (ed). Dordrecht: Springer Netherlands, pp. 147–178.

809 Philipp, E. and Fabricius, K. (2003) Photophysiological stress in scleractinian corals in response  
810 to short-term sedimentation. *J Exp Mar Bio Ecol* **287**: 57–78.

811 Pollock, F.J., Lamb, J.B., Field, S.N., Heron, S.F., Schaffelke, B., Shedrawi, G., et al. (2014)  
812 Sediment and turbidity associated with offshore dredging increase coral disease prevalence  
813 on nearby reefs. *PLoS One* **9**: e102498.

814 Pruzzo, C., Huq, A., Colwell, R.R., and Donelli, G. (2005) Pathogenic *Vibrio* Species in the  
815 Marine and Estuarine Environment. In *Oceans and Health: Pathogens in the Marine*  
816 *Environment*. Belkin, S. and Colwell, R.R. (eds). Boston, MA: Springer US, pp. 217–252.

817 Quast, C., Pruesse, E., Yilmaz, P., Gerken, J., Schweer, T., Yarza, P., et al. (2013) The SILVA  
818 ribosomal RNA gene database project: improved data processing and web-based tools.

819 *Nucleic Acids Res* **41**: D590–6.

820 Riegl, B. and Branch, G.M. (1995) Effects of sediment on the energy budgets of four  
821 scleractinian (Bourne 1900) and five alcyonacean (Lamouroux 1816) corals. *J Exp Mar Bio*  
822 *Ecol* **186**: 259–275.

823 Sañudo-Wilhelmy, S.A., Kustka, A.B., Gobler, C.J., Hutchins, D.A., Yang, M., Lwiza, K., et al.  
824 (2001) Phosphorus limitation of nitrogen fixation by *Trichodesmium* in the central Atlantic  
825 Ocean. *Nature* **411**: 66–69.

826 Sharma, S., Sachdeva, P., and Viridi, J.S. (2003) Emerging water-borne pathogens. *Appl*  
827 *Microbiol Biotechnol* **61**: 424–428.

828 Sheridan, C., Baele, J.M., Kushmaro, A., Fréjaville, Y., and Eeckhaut, I. (2014) Terrestrial runoff  
829 influences white syndrome prevalence in SW Madagascar. *Mar Environ Res* **101**: 44–51.

830 Shinn, E.A., Smith, G.W., Prospero, J.M., Betzer, P., Hayes, M.L., Garrison, V., and Barber,  
831 R.T. (2000) African dust and the demise of Caribbean Coral Reefs. *Geophys Res Lett* **27**:  
832 3029–3032.

833 Siegesmund, M.A., Johansen, J.R., Karsten, U., and Friedl, T. (2008) COLEOFASCICULUS  
834 GEN. NOV. (CYANOBACTERIA): MORPHOLOGICAL AND MOLECULAR CRITERIA FOR  
835 REVISION OF THE GENUS MICROCOLEUS GOMONT(1). *J Phycol* **44**: 1572–1585.

836 Silva, J., Leite, D., Fernandes, M., Mena, C., Gibbs, P.A., and Teixeira, P. (2011)  
837 *Campylobacter* spp. as a Foodborne Pathogen: A Review. *Front Microbiol* **2**: 200.

838 Solo-Gabriele, H.M., Wolfert, M.A., Desmarais, T.R., and Palmer, C.J. (2000) Sources of  
839 *Escherichia coli* in a coastal subtropical environment. *Appl Environ Microbiol* **66**: 230–237.

840 Soo, R.M., Skennerton, C.T., Sekiguchi, Y., Imelfort, M., Paech, S.J., Dennis, P.G., et al. (2014)  
841 An expanded genomic representation of the phylum cyanobacteria. *Genome Biol Evol* **6**:  
842 1031–1045.

843 Sussman, M., Willis, B.L., Victor, S., and Bourne, D.G. (2008) Coral Pathogens Identified for  
844 White Syndrome (WS) Epizootics in the Indo-Pacific. *PLoS One* **3**: e2393.

845 Sutherland, K.P., Porter, J.W., and Torres, C. (2004) Disease and immunity in Caribbean and  
846 Indo-Pacific zooxanthellate corals. *Mar Ecol Prog Ser* **266**: 273–302.

847 Sutherland, K.P., Shaban, S., Joyner, J.L., Porter, J.W., and Lipp, E.K. (2011) Human pathogen  
848 shown to cause disease in the threatened elkhorn coral *Acropora palmata*. *PLoS One* **6**:  
849 e23468.

850 Vizcaino, M.I., Johnson, W.R., Kimes, N.E., Williams, K., Torralba, M., Nelson, K.E., et al.  
851 (2010) Antimicrobial resistance of the coral pathogen *Vibrio coralliilyticus* and Caribbean  
852 sister phylotypes isolated from a diseased octocoral. *Microb Ecol* **59**: 646–657.

853 Voss, J.D. and Richardson, L.L. (2006) Coral diseases near Lee Stocking Island, Bahamas:  
854 patterns and potential drivers. *Dis Aquat Organ* **69**: 33–40.

855 Wang, B., Yang, Y., Ding, Q.-H., Murakami, H., and Huang, F. (2010) Climate control of the  
856 global tropical storm days (1965-2008): CLIMATE CONTROL OF TROPICAL STORM  
857 DAYS. *Geophys Res Lett* **37**:

858 Weber, M., de Beer, D., Lott, C., Polerecky, L., Kohls, K., Abed, R.M.M., et al. (2012)  
859 Mechanisms of damage to corals exposed to sedimentation. *Proc Natl Acad Sci U S A* **109**:  
860 E1558–67.

861 Weiskel, P.K., Howes, B.L., and Heufelder, G.R. (1996) Coliform Contamination of a Coastal  
862 Embayment: Sources and Transport Pathways. *Environ Sci Technol* **30**: 1872–1881.

863 Wetz, M.S. and Paerl, H.W. (2008) Estuarine Phytoplankton Responses to Hurricanes and  
864 Tropical Storms with Different Characteristics (Trajectory, Rainfall, Winds). *Estuaries*  
865 *Coasts* **31**: 419–429.

866 Willis, A. and Bunge, J. (2015) Estimating diversity via frequency ratios. *Biometrics* **71**: 1042–  
867 1049.

868 Willis, A., Bunge, J., and Whitman, T. (2017) Improved detection of changes in species richness  
869 in high diversity microbial communities. *J R Stat Soc C* **66**: 963–977.

870 Wilson, B., Aeby, G.S., Work, T.M., and Bourne, D.G. (2012) Bacterial communities associated  
871 with healthy and *Acropora* white syndrome-affected corals from American Samoa. *FEMS*  
872 *Microbiol Ecol* **80**: 509–520.

873 Witt, V., Wild, C., and Uthicke, S. (2012) Terrestrial runoff controls the bacterial community  
874 composition of biofilms along a water quality gradient in the Great Barrier Reef. *Appl*  
875 *Environ Microbiol* **78**: 7786–7791.

876 Wooldridge, S.A. (2009) Water quality and coral bleaching thresholds: formalising the linkage  
877 for the inshore reefs of the Great Barrier Reef, Australia. *Mar Pollut Bull* **58**: 745–751.

878 Wu, J. and Boyle, E.A. (1998) Determination of iron in seawater by high-resolution isotope  
879 dilution inductively coupled plasma mass spectrometry after Mg(OH)<sub>2</sub> coprecipitation. *Anal*  
880 *Chim Acta* **367**: 183–191.

881 Wu, J., Chung, S.-W., Wen, L.-S., Liu, K.-K., Chen, Y.-L.L., Chen, H.-Y., and Karl, D.M. (2003)  
882 Dissolved inorganic phosphorus, dissolved iron, and Trichodesmium in the oligotrophic  
883 South China Sea : PHOSPHATE, IRON, AND NITROGEN FIXATION IN THE SOUTH  
884 CHINA SEA. *Global Biogeochem Cycles* **17**: 8–1–8–10.

885 Yamano, H. and Watanabe, T. (2016) Coupling Remote Sensing and Coral Annual Band Data  
886 to Investigate the History of Catchment Land Use and Coral Reef Status. In *Coral Reef*  
887 *Science: Strategy for Ecosystem Symbiosis and Coexistence with Humans under Multiple*  
888 *Stresses*. Kayanne, H. (ed). Tokyo: Springer Japan, pp. 47–53.

889 Yamazaki, A., Watanabe, T., Tsunogai, U., Hasegawa, H., and Yamano, H. (2015) The coral  
890  $\delta^{15}\text{N}$  record of terrestrial nitrate loading varies with river catchment land use. *Coral Reefs*.

891 Yeo, S.K., Huggett, M.J., Eiler, A., and Rappé, M.S. (2013) Coastal bacterioplankton community  
892 dynamics in response to a natural disturbance. *PLoS One* **8**: e56207.

893 Zhang, J.-Z., Kelble, C.R., Fischer, C.J., and Moore, L. (2009) Hurricane Katrina induced  
894 nutrient runoff from an agricultural area to coastal waters in Biscayne Bay, Florida. *Estuar*  
895 *Coast Shelf Sci* **84**: 209–218.

896 Zhou, W., Yin, K., Harrison, P.J., and Lee, J.H.W. (2012) The influence of late summer  
897 typhoons and high river discharge on water quality in Hong Kong waters. *Estuar Coast*  
898 *Shelf Sci* **111**: 35–47.

899 Zimmer, B.L., May, A.L., Bhedi, C.D., Dearth, S.P., Prevatte, C.W., Pratte, Z., et al. (2014)  
900 Quorum sensing signal production and microbial interactions in a polymicrobial disease of  
901 corals and the coral surface mucopolysaccharide layer. *PLoS One* **9**: e108541.

902 R Core Team (2018). R: A language and environment for statistical computing. R Foundation for  
903 Statistical Computing, Vienna, Austria. URL <https://www.R-project.org/>.

904  
905

## 906 **Figure legends**

907 **Figure 1. Location of the study area** A) Map locating Okinawa Island in the East China  
908 Sea. B) Map showing the location of the central-west coast of Okinawa Island. C)  
909 Location of the 4 nearshore sampling points in Onna-son, on the central-west  
910 coast of Okinawa Island.

911

912 **Figure 2. Precipitation (in mm day<sup>-1</sup>) and wind speed (m s<sup>-1</sup>) during the 2018**  
913 **typhoon season in Okinawa, Japan.** Data were collected with the  
914 meteorological station located at OIST Marine Science Station (26.510046 °N,  
915 127.871721 °E) from June through October, corresponding to the duration of the  
916 typhoon season in Okinawa. Bars represent the daily amount of rain (in mm);  
917 dashed black and red lines indicate daily mean and maximum wind speeds (in m  
918 s<sup>-1</sup>); shaded areas represent the two red soil pollution events monitored in this  
919 study: Tropical Storm Gaemi on June 16 and the super-typhoons Trami and  
920 Kong-Rey on September 29 and October 5. The dates when water samples were  
921 collected for chemical and DNA analyses are noted on the x-axis.

922  
923 **Figure 3. Temporal variation of physicochemical parameters before, during, and**  
924 **after storm events in June and October, 2018.** Bars represent the values of  
925 temperature (°C), turbidity (NTU), salinity (‰) and concentrations of micro- and  
926 macro-nutrient concentrations (NO<sub>2</sub><sup>-</sup>, NO<sub>3</sub><sup>-</sup>, NH<sub>4</sub><sup>+</sup>, PO<sub>4</sub><sup>3-</sup>, SiO<sub>2</sub> in μM; dFe in nM) at  
927 sampling sites A1–4 along the central west coast of Okinawa, Japan. Error bars  
928 represent one standard deviation of the mean from four replicates. Red dashed  
929 vertical lines represent the timing of major storms and associated red soil  
930 pollution events. Sampling dates when samples were also processed for  
931 metabarcoding analyses are indicated in bold on the x-axis. Temperature (°C),  
932 turbidity (NTU) and salinity (‰) measurements were taken with a CTD probe.  
933 Macro-nutrient concentrations were determined on a QuAAtro39 Continuous  
934 Segmented Flow Analyzer and dFe concentration was determined by ICP-MS  
935 after Mg(OH)<sub>2</sub> co-precipitation using the isotope dilution method (Wu and Boyle,  
936 1998).

937



938 **Figure 4. Relative abundance of bacterial phyla in field and mesocosm samples**  
939 **collected in June and October, 2018.** Each stacked bar represents the relative  
940 contribution of major bacterial phyla to the total community at one sampling  
941 location, in one red soil sample, or at one time point in mesocosms (mesocosm  
942 bars represent aggregate data from 4–5 replicates depending on month and  
943 treatment). Sampling stations (A)1–4 were sampled before, during, and after  
944 major storms affecting Okinawa in June and October 2018. In June, the storm  
945 affected Okinawa on 6/16, so that sampling on 6/13 was before the storm and  
946 sampling on 6/19 was afterward. In October, two super typhoons affected  
947 Okinawa on 9/28 and 10/05 so that 9/28 was before the event window, 10/01  
948 and 10/03 was during the event window, and 10/08 was afterward. Red soil  
949 samples are labeled with replicate numbers and were collected within a week of  
950 the storms in June and October. Red soil ( $200 \text{ mg L}^{-1}$ ) was added to treatment  
951 mesocosms immediately following the  $t_0$  sampling.

952  
953 **Figure 5. Principal component analysis (PCA) of Aitchison distances between**  
954 **bacterial community composition before, during, and after storm events in**  
955 **June (A) and October (B), 2018.** (A) June 13 was before the June storm, 6/16  
956 was during, and 6/19 was after. For the October storms (B), 9/28 was before the  
957 storms, 10/01 and 10/03 were between, and 10/08 was after. Samples collected  
958 during/between storm events separate from samples collected before and after  
959 storms on PC1 for both the June and October events.

960  
961 **Figure 6. Richness estimates for bacterial communities in red soil samples and**  
962 **surface water samples collected before, during, and after storm events in**  
963 **June (A) and October (B), 2018.** Red dashed vertical lines represent the timing

964 of major storms. In June (A), the red soil samples had significantly higher  
965 richness than the water samples collected before and after the storm, but not  
966 samples collected during the storm. In October (B), red soil samples had  
967 significantly higher richness than all water samples and richness was not  
968 significantly different in water samples collected before, during, or after the  
969 storms. Differences in richness were considered significant when  $p < 0.05$ .

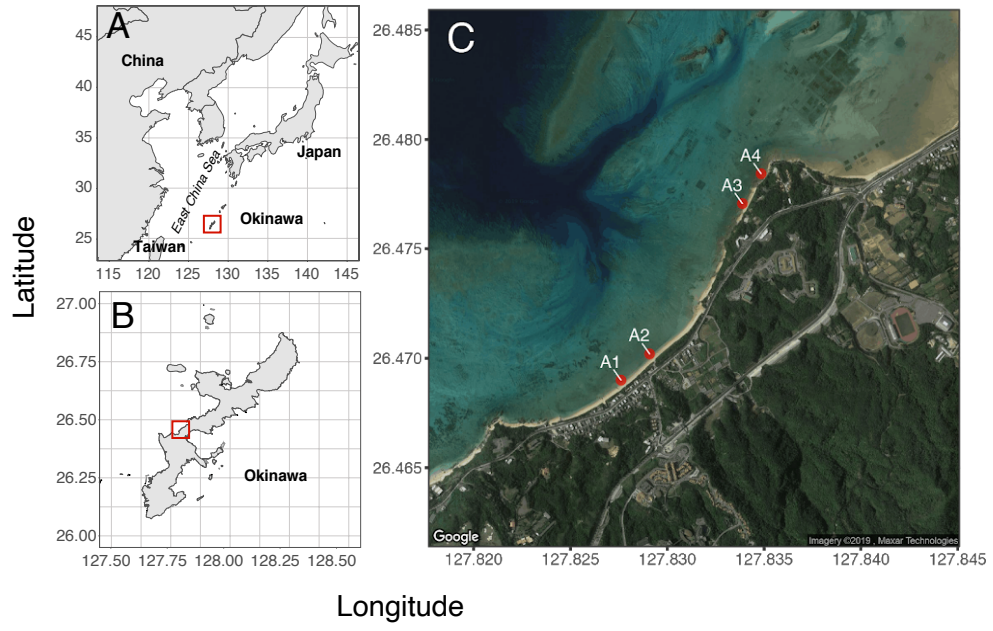
970

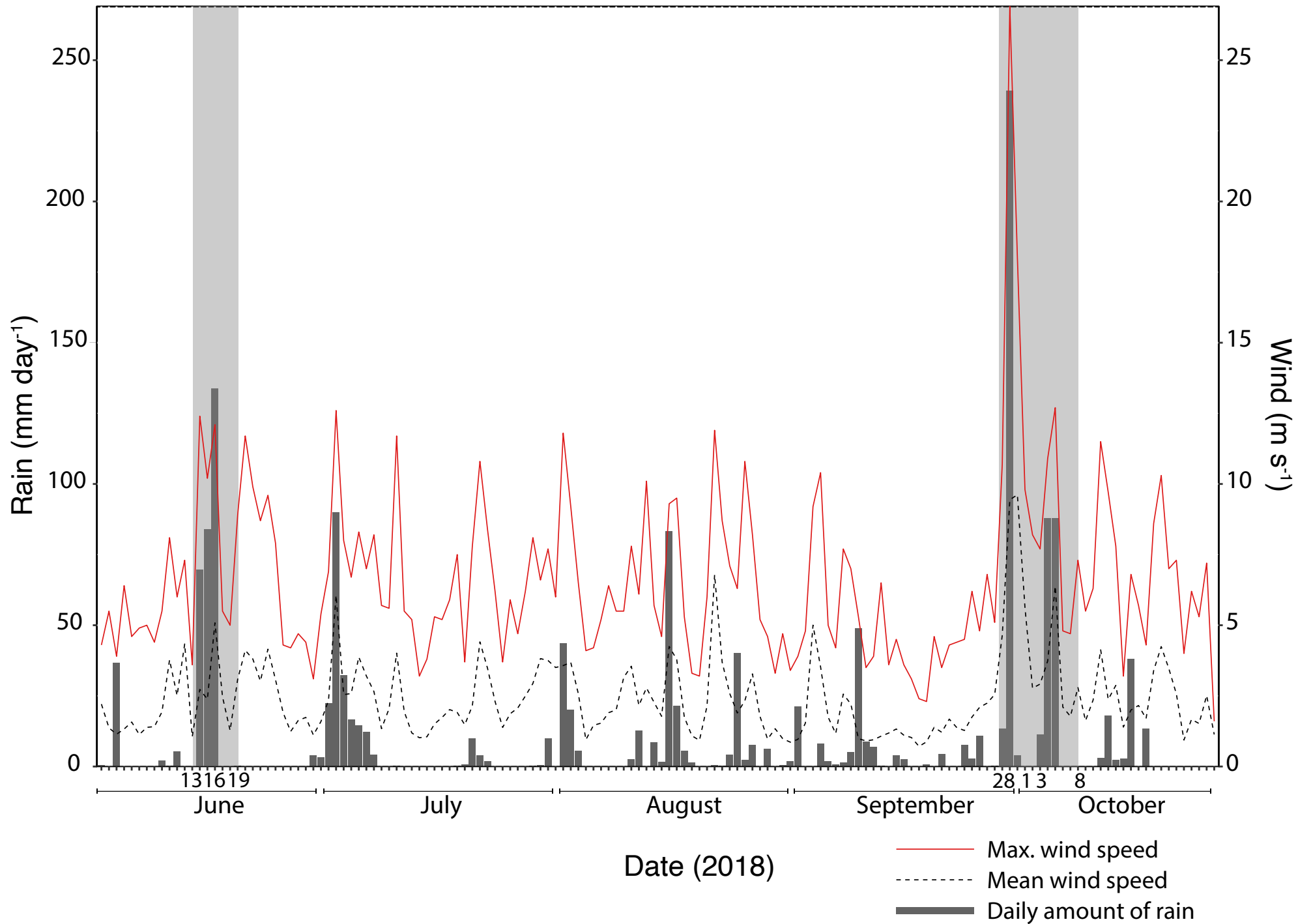
971 **Figure 7. Number of Amplicon Sequence Variants (ASVs) significantly**  
972 **differentially abundant in pairwise comparisons between sampling dates in**  
973 **June (A) and October (C) and log<sub>2</sub> Fold Change of individual ASVs in**  
974 **pairwise comparisons from before to during storms and from before to**  
975 **after storms in June (B) and October (D), 2018.** ASVs were considered  
976 significantly differentially abundant when the FDR adjusted  $p$ -value was less than  
977 0.05. ASVs that were also present in soil samples are colored red in panels A  
978 and B; no differentially abundant ASVs in pairwise tests for October samples  
979 were found to be present in October soil samples. Positive log<sub>2</sub>FoldChange  
980 values (x-axis, B, D) indicate higher abundance of ASVs during/between storms  
981 compared to before (J13 to J16, S28 to O01 + O03) or after storms compared to  
982 before (J13 to J19, S28 to O08). Differentially abundant ASVs are grouped by  
983 taxonomic order and orders are color coded by phylum so that colors correspond  
984 to Figure 4.

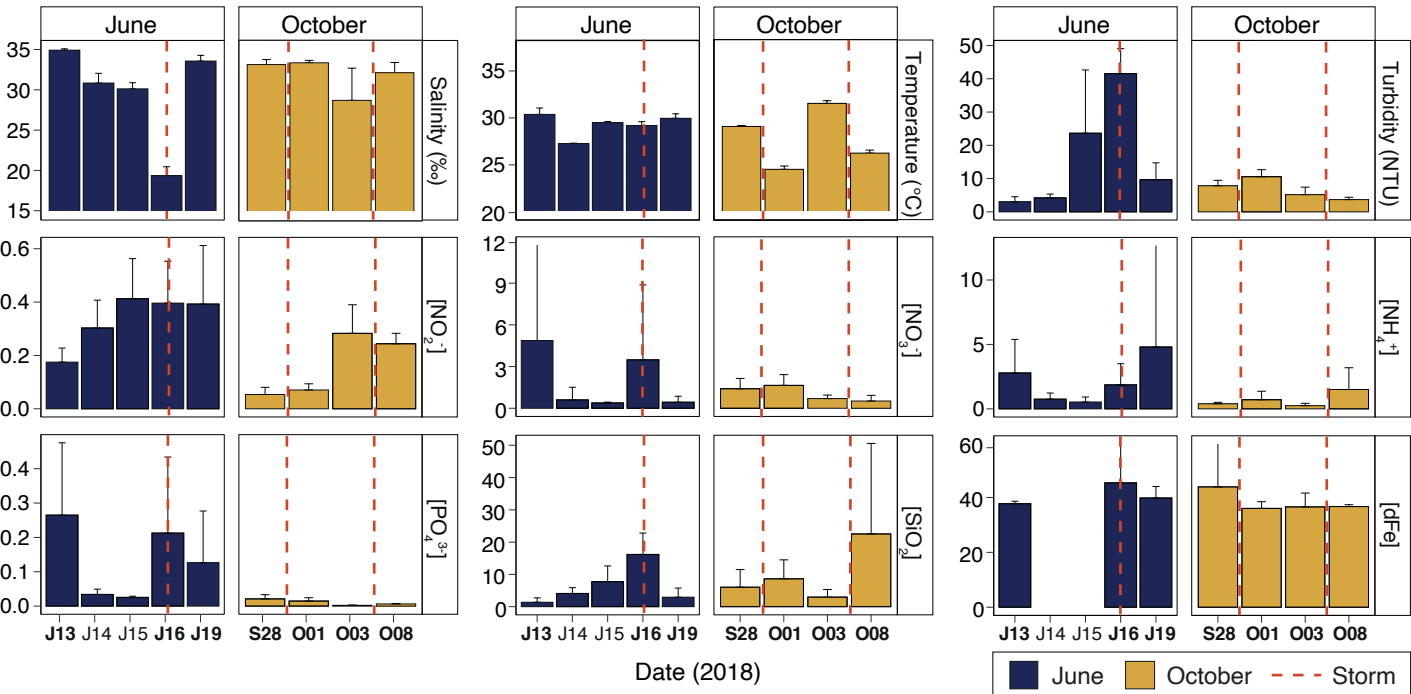
985

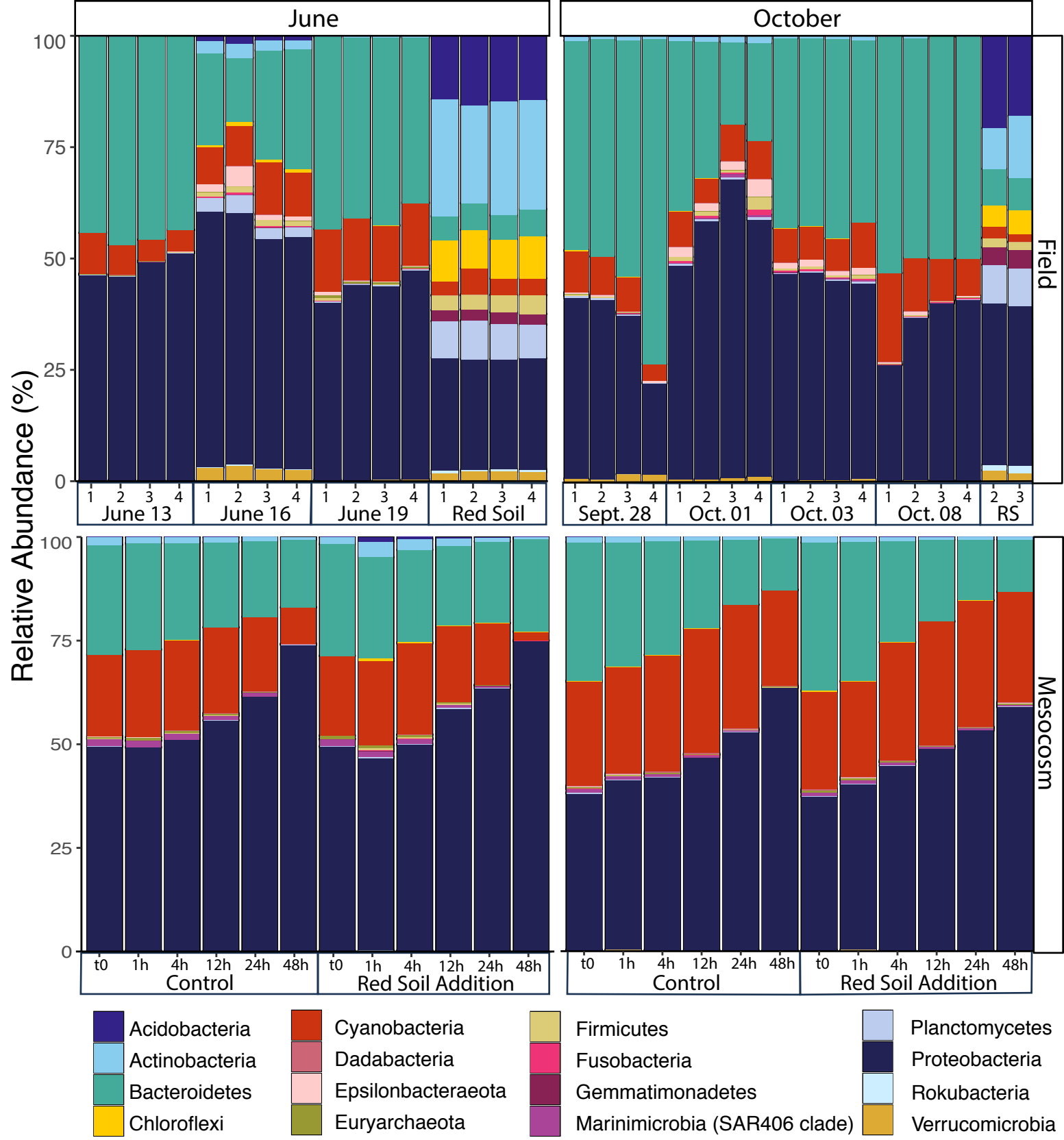
986

987

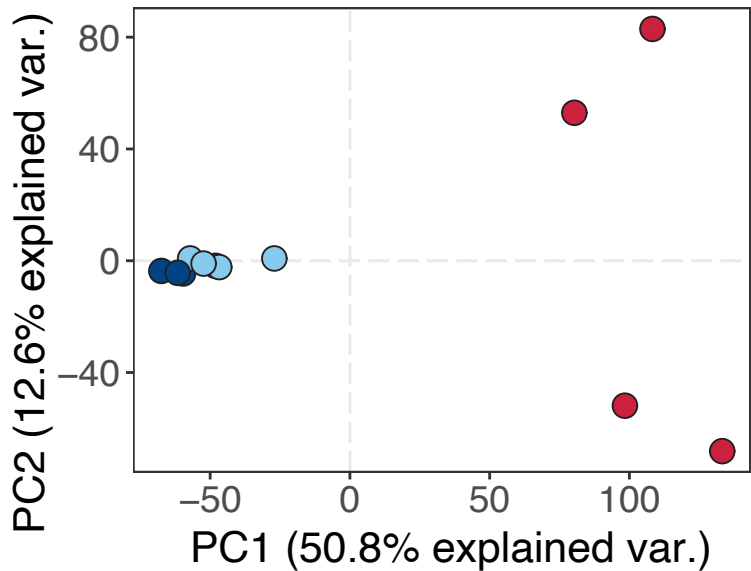






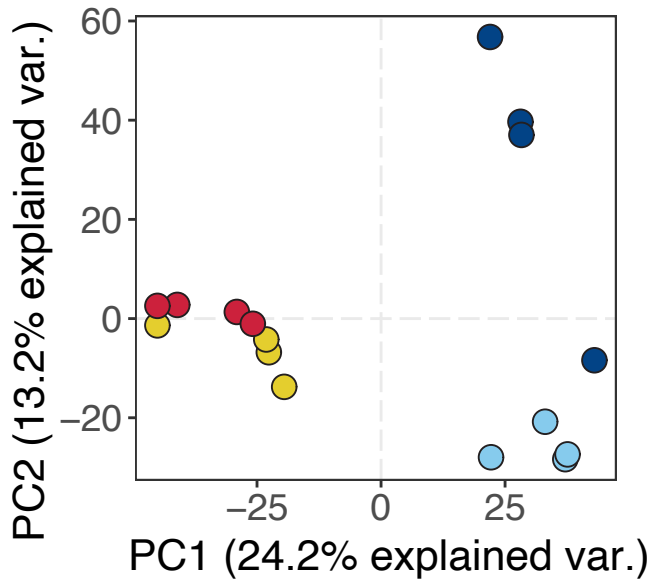


### A. June



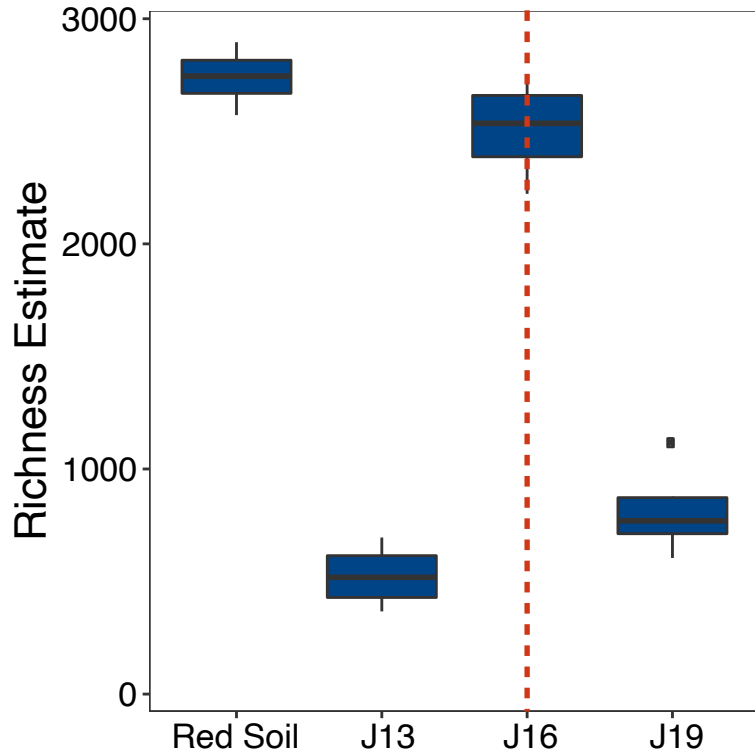
● 13-Jun ● 16-Jun ● 19-Jun

### B. October

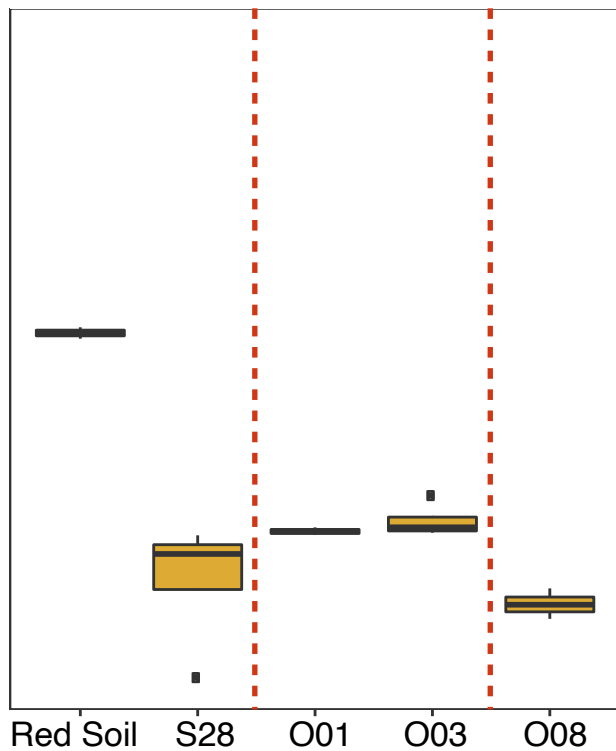


● 28-Sep ● 1-Oct ● 3-Oct ● 8-Oct

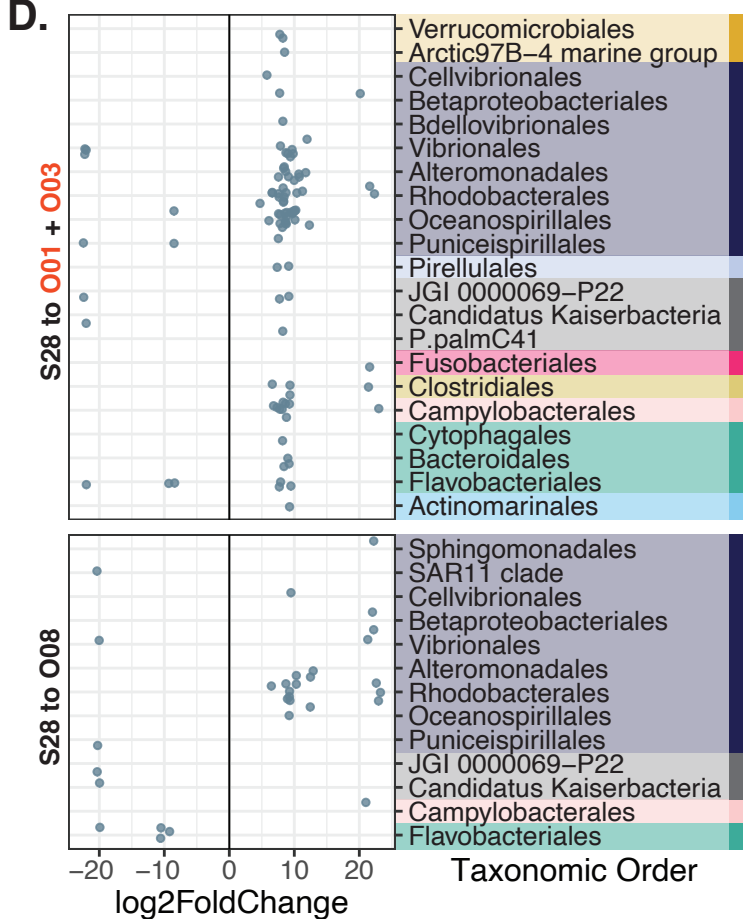
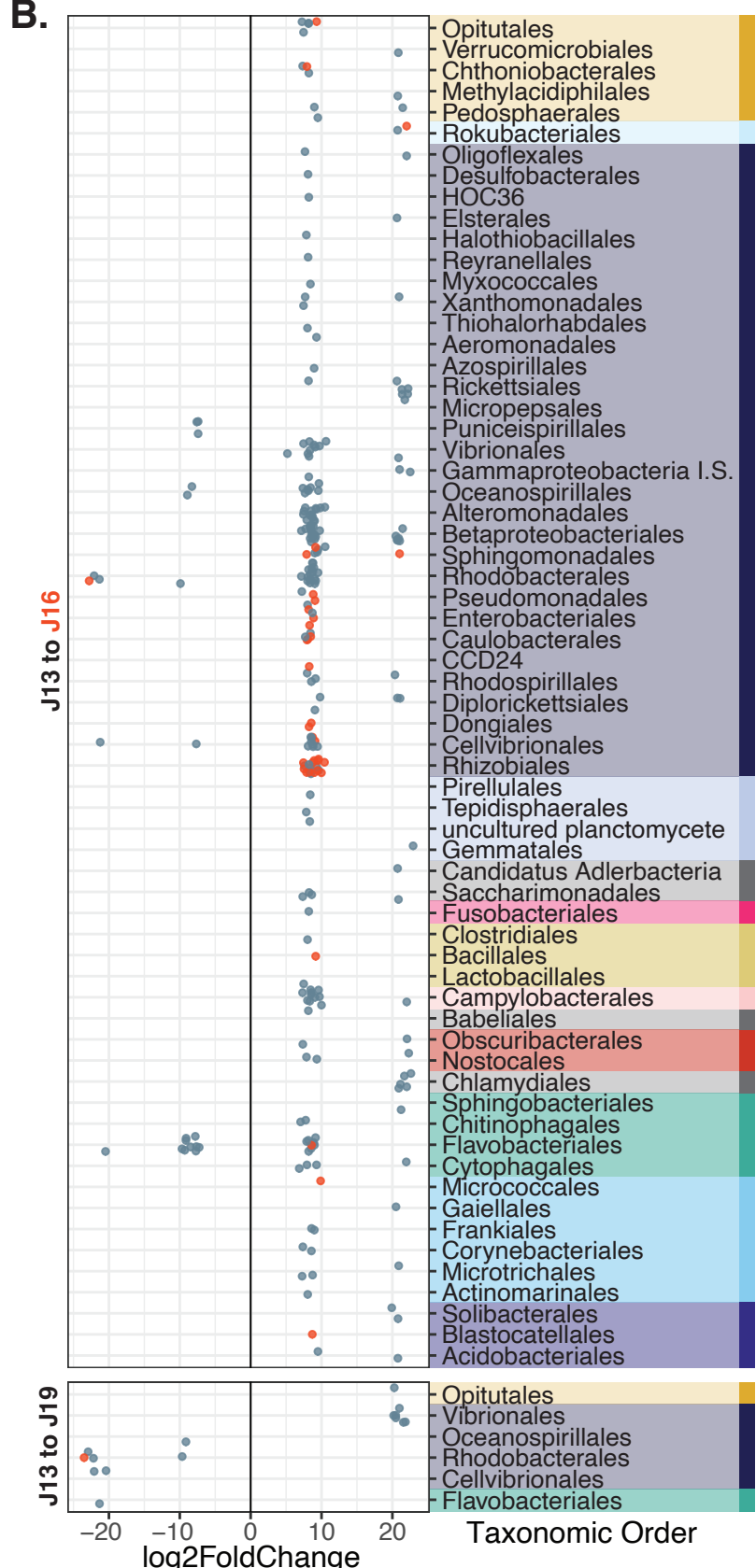
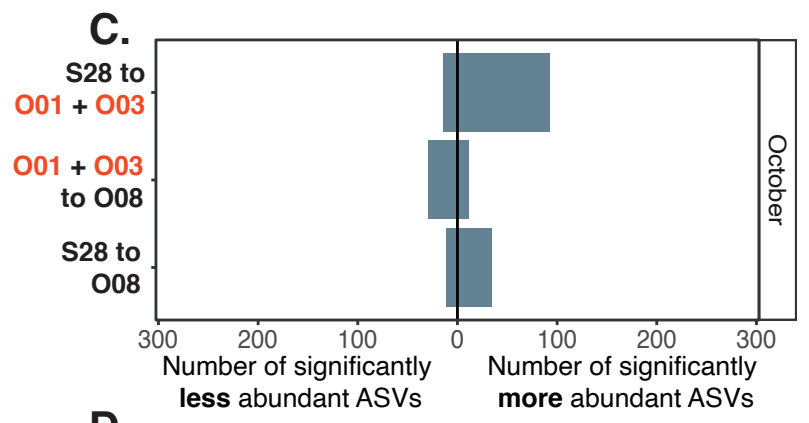
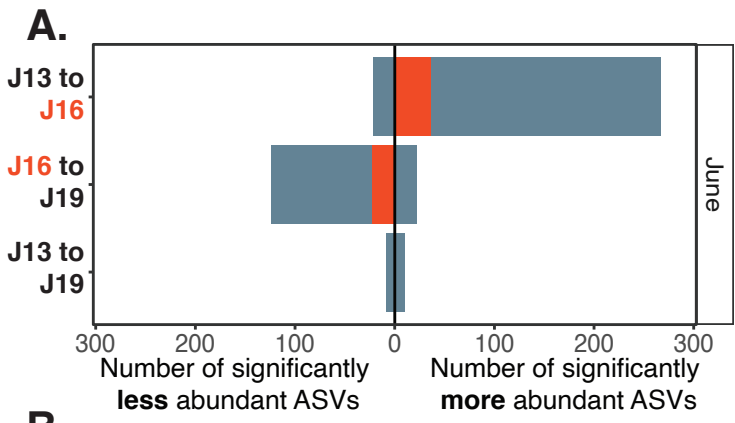
A. June



B. October







Decreased | Increased  
during/between | during/between (top panel)  
or after | or after (bottom panel)

● Not found in soil samples  
● Found in soil samples

Phylum:

Verrucomicrobia	Epsilonbacteraeota
Rokubacteria	Cyanobacteria
Proteobacteria	Bacteroidetes
Planctomycetes	Actinobacteria
Fusobacteria	Acidobacteria
Firmicutes	Other